FINAL REPORT

Man-Portable Magnetic Scalar Triangulation and Ranging System for Detection, Localization and Discrimination of UXO

SERDP Project MM-1511

November 2009

Dr. Roy F. Wiegert
NSWC-PC

This document has been approved for public release.

Strategic Environmental Research and Development Program

This report was prepared under contract to the Department of Defense Strategic Environmental Research and Development Program (SERDP). The publication of this report does not indicate endorsement by the Department of Defense, nor should the contents be construed as reflecting the official policy or position of the Department of Defense. Reference herein to any specific commercial product, process, or service by trade name, trademark, manufacturer, or otherwise, does not necessarily constitute or imply its endorsement, recommendation, or favoring by the Department of Defense.

Table of Contents

Executive Summary…….…… 1

Objective……..……. 5

Background……..……...… 6

Materials and Methods……...….....……..... 16

Results and Accomplishments……...…… 25

Concluding Summary......……...….. 43

List of References.....……..... 44

Appendices:

(A) List of technical publications, presentations and patents ....……..... 45

(B) Computer program listings .....……... 46

List of Acronyms and Symbols

ADC: Analog to digital converter
Am^2: Ampere x meter-squared (magnetic dipole moment = magnetic signature)
AUV: Autonomous Unmanned Vehicle
B_A: Magnetic anomaly field
C_T: Contraction (Frobenius norm) of magnetic gradient tensor
CPU: Central Processing Unit
DC: Direct current (used to denote static or near zero frequency fields, voltages or currents)
DD: Directional derivative.
DLC: Detection, Localization and Classification/discrimination
ESTCP: Environmental Security Technology Certification Program
G: Magnetic gradient tensor
GPS: Global Positioning System
GUI: Graphical User Interface
FY: Fiscal Year
Hz: Hertz (a unit of frequency = 1 cycle per second)
LSF: Least-squares-fit.
M: Magnetic dipole moment
MagSTAR: Magnetic Scalar Triangulation and Ranging
MCM: Mine Countermeasures
nT: nano Tesla = 10^{-9} Tesla
NSWC PCD: Naval Surface Warfare Center Panama City Division
PI: Principal Investigator
pp: Peak to peak
pT: Pico Tesla = 10^{-12} Tesla
R&D: Research and Development
rms: root mean square
SBC: Single Board Computer
SERDP: Strategic Environmental Research and Development Program
SON: Statement of need.
STAR: Scalar Triangulation and Ranging
T: Tesla, unit of magnetic induction field
T&E: Test and Evaluation
TFM: Triaxial Fluxgate Magnetometer
UBV: Underwater Bottom Vehicle
USPTO: United States Patent and Trademark Office
UXO: Unexploded Ordnance

List of Figures and Tables

Fig. 1. Illustration of the objective of Project MM-1511. 5
Fig. 2. Theoretical representation of the C_T field from a magnetic dipole target 11
Fig 3. Magnetic Scalar Triangulation and Ranging (STAR) Concept 11
Fig. 4. Cluttered gradient contraction field. 12
Fig. 5. Preferred geometry for a MagSTAR: a STAR-Cube 13
Fig. 6. Basic design and operation of a STAR Sensor. 13
Fig. 7. Geometrical relation between triangulation parameters. 14
Fig. 8. Prototype 2-D "UBV-STAR" gradiometer and data. 15
Fig. 9. Sketch of portable STAR Sensor design. 17
Fig. 10. Important hardware elements of portable STAR Sensor 18
Fig. 11. Sensor Support Structure (SSS). 18
Fig. 12. Signal Processing and Control (electronics box). 19
Fig. 13. Orientation sensor. 20
Fig. 14. High-level flow diagram of MagSTAR computer program. 21
Fig 15. Signal flow diagram for prototype STAR system. 23
Fig. 16. Prototype Man-Portable STAR Sensor. 23
Fig. 17. Simulations of STAR sensor's DLC performance.. 26
Fig. 18. Noise spectrum of a ***B***-field sensing element. 27
Fig. 19. Reduction of motion noise effects. 29
Fig. 20. View of MagSTAR being carried for field testing. 31
Fig. 21. Procedure for field tests. 31
Fig. 22. Gradient tensor data and screenshot from operator's display. 32
Fig. 23. Complete set of gradient data (horizontal sweep past target). 34
Fig. 24. Complete set of gradient data (vertical sweep past target). 35
Fig. 25. Intermittent malfunction of a *B*-field sensing element. 37
Fig. 26. Improved localization and classification using DD/LSF algorithm. 40
Fig. 27. Magnitudes of target range and magnetic signature using DD/LSF. 40
Fig. 28. Results from DD/LSF from linear (right to left) sweep past target. 41
Fig. 29. Screenshot from application of DD/LSF to field test data. 41
Fig. 30. Representation of progress toward objective described in Fig. 1. 43

Acknowledgements

Project MM-1511 and it's accomplishments were made possible by the sponsorship of the Strategic Environmental Research and Development Program (SERDP) and the careful attention, support and encouragement provided by SERDP and the SERDP Staff. In particular, the project has benefited from the support and constructive feedback of Drs Jeff Marqusee, Anne Andrews and Herb Nelson. The project's research and development work was performed by a team of researchers and engineers at Naval Surface Warfare Center Panama City: John Oeschger dedicated truly outstanding programming and field test support, Eric Tuovila provided the MagSTAR sensor's original signal processing/sensor control unit and Rob Parker developed the carbon-fiber sensor support structure. Richard Brantley contributed a very effective, upgraded dual-core signal processor and control unit.

Executive Summary

Environmental Problem Addressed

Project MM-1511 focused on development of an improved magnetic sensor system technology to address the environmental problem posed by hidden and buried Unexploded Ordnance (UXO) such as unexploded bombs, artillery shells, mines, etc., at sites such as Formerly Used Defense Sites and other closed or active weapons test ranges. In particular, the project's Research and Development (R & D) effort addresses the need to develop improved man-portable sensing platforms and advanced signal processing technologies that will more efficiently and cost-effectively perform detection and discrimination of UXO. The need for improved portable sensing and discrimination technologies is described in the Strategic Environmental Research and Development Program (SERDP) Statements of Need (SON) numbers UXSON-06-04 "Development of Handheld and Man-Portable Platforms Supporting Geophysical Surveys of Unexploded Ordnance Contaminated Sites" and MMSON-08-04 "Advanced Technologies for Detection, Discrimination and Remediation of Military Munitions." Specifically, MM-1511 addresses the need for development of portable and/or advanced sensors and signal processing technologies that can more effectively be applied to the cleanup of Department of Defense (DoD) munitions-contaminated sites with difficult geology, terrain and vegetation, and complex ordnance and clutter distributions. The R&D effort focused on development of: 1) an improved man-portable magnetic sensing technology for real-time, point-by-point Detection, Localization and Classification (DLC) of magnetic UXO, and 2) new signal processing approaches that will allow the portable sensor and other future sensor systems to perform more effective DLC of UXO in magnetically cluttered areas.

Scientific Questions Explored

Project MM-1511 performed R&D of a new magnetic anomaly sensing-based technology concept for localization/classification of ferrous UXO-type targets. The new technology measures and processes scalar magnitudes of the gradients of the DC magnetic anomaly fields that emanate from magnetically polarized ferrous objects. In the context of this sensor development effort, the term DLC means that the new technology will: i) detect the presence of the ferrous objects, ii) determine the object's vector location, and iii) measure the object's magnetic dipole moment vector. As discussed in more detail in the Background section, here the term "classification" signifies accurate measurements of the three dimensional (3-D) vector components of a ferrous object's magnetic dipole moment.

According to tensor theory, the magnitude (Frobenius norm; also denoted as "gradient contraction") of the gradient tensor of a vector field is a rotationally invariant scalar quantity. Furthermore, electromagnetics theory indicates that the magnitude of the tensor that represents the gradient of the magnetostatic dipole field of a magnetically polarized object has a robust mathematical/geometrical form that is analogous to that of a central potential field that is centered on the source of the dipole field, that is, on the magnetic object or ferrous UXO. Therefore, a multi-tensor magnetic sensing approach that exploits the mathematical and geometrical properties of the tensor magnitude field should be

resistant to the effects of sensor platform motion and be capable of true real time DLC of magnetic targets. In particular, these theoretical considerations indicate that gradient contraction data from a properly designed, three-dimensional multi-tensor magnetic gradiometer can be used to perform point-by-point (standoff) localization and classification of magnetic UXO by applying a unique, motion-noise-resistant magnetic Scalar Triangulation and Ranging (STAR) concept.

In summary the scientific questions explored by Project MM-1511 were to determine the validity of the theoretical STAR concept and to verify its potential advantages for application to highly maneuverable sensing platforms for high-speed, point-by-point DLC of magnetic targets. The project's specific technological goal was the development of a man-portable magnetic STAR (MagSTAR) sensor system for near real-time, point by point DLC of ferrous UXO in environments with multiple UXO-type targets and magnetic clutter.

Cumulative Results: FY06-FY08.

Project MM-1511 was initially funded by SERDP during fiscal years 2006-2007 (i.e., FY06-07) to develop and demonstrate a man-portable magnetic sensor based on the magnetic STAR concept. Subsequent to the successful demonstration of the MagSTAR technology in FY07 the project's funding was extended through FY08 and R&D work with the objective of developing the technology for use in magnetically cluttered environments continued until FY08 funds were fully expended in the second quarter of FY09. In outline, per fiscal year the project's cumulative results are:

- FY 2006: Design, construction and preliminary tests (at Naval Surface Warfare Center Panama City Division (NSWC PCD)) of the first prototype man-portable MagSTAR sensor system. The work was performed by two physicists, an electrical engineer and a mechanical engineer. R&D results included theoretical modeling of STAR sensor performance, development of algorithms (coded in MATLAB) for data acquisition, target localization and residual motion noise compensation, design and construction of the first man-portable STAR sensor and laboratory tests and field tests of MagSTAR hardware and software subsystems such as field-sensing elements and signal processing elements.
- FY 2007: Completion of construction, initial tests, and evaluation of preliminary field of the of the prototype MagSTAR sensor technology. Cumulative results for the project in 2007 include:
  - Performance of field tests that very successfully demonstrated: 1) the basic validity of the theoretical STAR concept and 2) the unique advantages of the STAR technology for real-time, point-by-point Detection, Localization and Classification (DLC) of magnetic objects.
  - Improvements to the prototype man-portable sensor:
    + Completion of a completely portable, battery-powered self-contained system.
    + Integration of a novel head-mounted display for the sensor operator and a graphical user interface for user-friendly operation of the sensor system.
    + Development of improved algorithms for real-time motion-noise compensation and high speed DLC of magnetic targets.
  - Experimental observation and preliminary measurements of the adverse effects of temperature changes on sensor system performance.

- FY 2008: Optimization, including a major upgrade of the signal processing system, of the prototype MagSTAR sensor and development of improved signal processing algorithms for more accurate point-by-point localization and discrimination of magnetic targets in magnetically cluttered areas. Cumulative results for the project in 2008 (through second quarter FY09) include:
  - Major upgrade of signal processing system including:
    + Replacement of the MagSTAR sensor's trouble-prone Pentium III type single board computer (SBC)-based data processing system with a much more effective Pentium Core-Duo (dual-core) 64-bit parallel processor capable of running the more advanced STAR-type signal processing algorithms that are needed for discrimination of multiple targets in magnetically cluttered environments.
    + Development of improved signal processing and control unit (electronics box) with better Input/Output (I/O) circuitry and more powerful batteries for the upgraded, dual-core SBC.
    + Development of C-based data acquisition software to reduce data dropouts that seem to be related to the MATLAB-based data acquisition code.
  - Development of new DLC algorithms including a directional derivative (DD) approach and a least squares fit (LSF) method that perform more accurate target localization completely independently of sensor platform orientation. A combination of DD plus LSF was used to eliminate the "asphericity errors" that are inherent to the original STAR algorithms.
  - Initial development of algorithms that use higher order gradients concurrently with the original STAR's first order gradients to provide an improved "through the sensor" modality for discrimination of UXO in cluttered environments..

In 2007 the project passed its Go/No-Go milestone when the hand-carried man-portable sensor prototype successfully demonstrated proof-of-principle of the magnetic STAR concept and clearly demonstrated the technology's advantages for motion-noise-resistant, high-speed, point-by-point standoff Detection, Localization and Classification (DLC) of magnetic targets. Field tests of the prototype STAR Sensor system, while being hand-carried by a single individual, consistently demonstrated near real-time (within a total system delay of about 3 seconds) point-by-point DLC of magnetic targets at ranges of five to seven meters from a 14.5 amp x meter-squared (Am^2) magnetic dipole target that was used simulate the UXO signature of a medium-sized bomb. The prototype MagSTAR sensor that achieved these results represents the worlds first successful man-portable magnetic sensor system technology for real-time point-by-point DLC of magnetic targets. In 2008 engineering issues such as mechanical instabilities and field-sensing element drift due to thermal effects have limited the technology's DLC range to about 60% of its theoretical range. These range-reducing effects have been characterized and technically sound approaches for mitigating the effects have been identified.

Subsequent to the demonstration of the basic validity and advantages of the magnetic STAR concept, in FY 07-08 and early FY09 Project MM-1511 primarily focused on refinement of the sensor system's hardware and software in order to address the problem of localization and discrimination of UXO in magnetically cluttered environments. In the latter part of 2007 and early FY08 progress was hampered by hardware problems due to malfunctions of the sensor system's single board computer (SBC) and an intermittent

malfunction of a magnetic field-sensing element. A more serious delay occurred when the project's key co-performer/ computer programmer left civil service to work for private industry. The processes of repair/ replacement of malfunctioning equipment and integration of new personnel resulted in reduced progress toward full development of the MagSTAR technology. However, as discussed in more detail in this report's Results and Accomplishments section the project's R&D work has succeeded in development of a prototype MagSTAR technology that when fully optimized will provide the UXO remediation community new magnetic sensing system technology for faster, more efficient detection, localization and classification/discrimination (DLC).

As part of an effort to communicate the results of this SERDP-sponsored new technology to the user community, multiple presentations and papers on the STAR Technology were delivered at five international conferences and several major symposia/workshops. Also, three patent applications on the STAR technology were filed with the United States Patent and Trademark Office. A list of presentations, papers and patent applications is included in Appendix A.

Potential future applications of the research and/or technology.

In addition to the MagSTAR technology's potential value for UXO-related geophysical surveys, potentially it also will provide an enabling technology for important Department of Defense (DoD) applications such as Explosive Ordnance Disposal (EOD) and Mine Countermeasures (MCM). Furthermore, the technology also will be readily adaptable to a wide range of military, commercial and scientific geophysical survey applications involving high-mobility sensing platforms such as robotic ground vehicles and unmanned aerial vehicles.

Objective

The Project's primary goal was the development of a new man-portable magnetic sensing technology for real-time, point-by-point standoff Detection, Localization and Classification/Discrimination (DLC) of ferrous UXO. Fig. 1 illustrates a notional concept of operations showing how the man-portable sensor would be used to locate buried UXO.

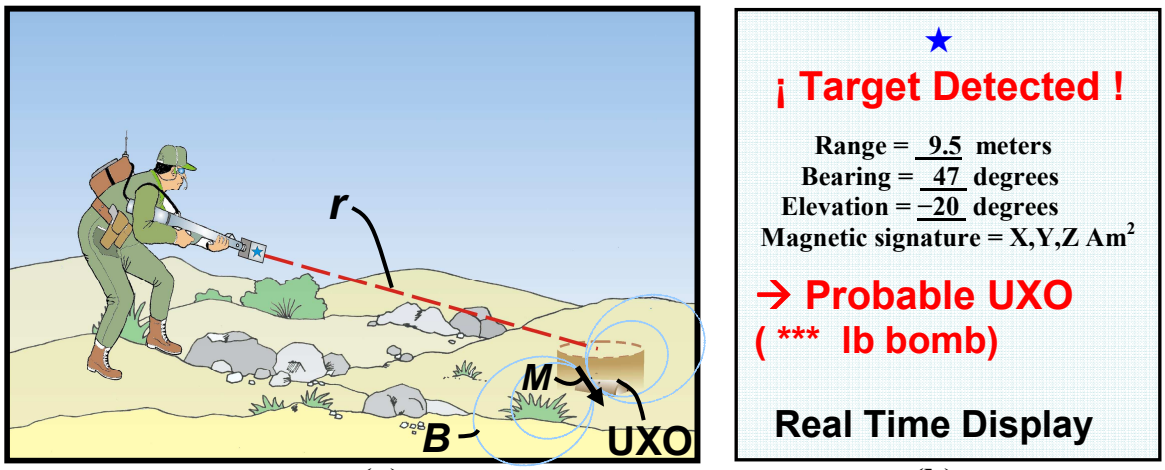

(a) **(b)**

Fig. 1. Notional concept of operations illustrating the objective of the STAR project.
(a) The sensor operator carries the man-portable magnetic sensor in the vicinity of buried UXO. The sensor automatically and in near-real-time (i.e., on the order of a second (s)) measures the UXO's field (***B***) and calculates its vector location (***r***) and its vector magnetic dipole moment (***M***). The 3-D components of the ***M***-vector constitute a magnetic signature that can be used classify the hidden target as UXO-like or not UXO-like.
(b) The UXO's location and magnetic signature data are displayed for the operator in near real-time. The sensor system would determine the probable classification of the buried target by comparing the magnitude and direction of the magnetic signature vector with, e.g., a look-up table correlating UXO types with their corresponding ***M***-values. In this notional concept the ***M*** vs. UXO table would be stored in the sensor's onboard signal processor.

Prior to Project MM-1511, there was no man-portable magnetic sensing technology capable of achieving true real-time point by point DLC of magnetic targets. To achieve this important technical objective, the project developed a prototype man-portable sensor based on a novel Magnetic Scalar Triangulation and Ranging (STAR) concept for high speed measurements of the vector location and magnetic signature of magnetic targets. Consequently, the project's specific technical objective was:

- The design, construction and demonstration of a completely portable, motion noise resistant magnetic gradient sensing system (STAR-type gradiometer) that easily can be carried by an individual operator and in near real time provide the operator with a point by point, on the fly, indication of the DLC parameters (e.g., range, bearing, elevation and magnetic signature) of magnetic UXO.

Background

Problem addressed by this project's technology.

The prototype magnetic sensing technology that was developed by this project addresses a Department of Defense (DoD) need for an improved mobile magnetic sensing technology that can perform more effective Detection, Localization and Classification (DLC) of magnetic UXO (e.g., bombs, artillery shells, etc.) and other magnetic targets located in munitions-contaminated sites with difficult geology, terrain and vegetation, and complex ordnance and clutter distributions. Notwithstanding the need (and potentially large commercial market) for a more efficient, high-mobility magnetic sensing technology, prior to the prototype sensor development work performed during Project MM-1511 no man-portable magnetic sensing technology had demonstrated a capability for real-time, point by point standoff DLC of magnetic targets.

In principle, magnetic Unexploded Ordnance (UXO) can be detected, localized and classified by using passive magnetic sensing systems that measure the UXO's static magnetic anomaly field. Since the magnetic signatures are little affected by intervening media such as nonmagnetic soil, foliage, water, etc, magnetic sensors can locate buried UXO that would remain hidden to other sensor technologies. However, the efficacy of conventional magnetic sensing technologies (e.g., scalar total field magnetometry and tensor gradiometry) for DLC of UXO has been limited by the effects of sensor motion noise in the Earth's magnetic field and sensor platform-signature noise.

Although scalar total field magnetometers can provide relatively good immunity to sensor motion noise they can not provide accurate point by point target DLC information. In principle, tensor gradiometers can accurately localize and classify targets. In practice, however, their use for mobile sensing applications heretofore has required sensing platform motion to be rather impractically constrained to proceed along straight-line paths with very little change in orientation. For example, tensor gradiometry using superconducting sensors onboard relatively large, stable platforms has been demonstrated at NSWC-PCD in several Office of Naval Research (ONR)-sponsored R & D projects for mine countermeasures and also in the SERDP-sponsored "Mobile Underwater Debris Detection System (MUDDS)" for detection of UXO [1]. In a test of the MUDDS in Choctawhatchee Bay, Florida, the system located and magnetically classified UXO-type targets with magnetic dipole signatures characteristic of 250 pound bombs. Visual verification of some of the UXO-type targets' was performed by Navy Divers. However, complete verification of all targets was impeded by limitations of the handheld total-field-type magnetic sensors that the Divers used for target localization.

NSWC PCD also has performed considerable R & D work on conventional tensor gradiometry using room-temperature fluxgate sensors and progress has been made toward addressing the technical issues related to tensor gradiometry [2]. However, the adverse effects of platform motion noise have continued to impede the development of a truly practical magnetic tensor gradiometer technology for highly mobile sensing platforms. The need to overcome the limitations of conventional technologies motivated the development of a unique new Magnetic Scalar Triangulation and Ranging (STAR or MagSTAR) approach to tensor gradiometry.

Tensor gradiometry and the Scalar Triangulation and Ranging (STAR) concept

The following technical background is included for convenience in defining the basic concepts that relate to magnetic tensor gradiometry and the MagSTAR's approach to localization and classification of magnetic targets. More detailed presentations of these concepts can be found in references [3-8]. The use of magnetic sensors to determine the vector components of a magnetic target's location vector $\boldsymbol{r}$ [m] and its magnetic dipole signature $\boldsymbol{M}$ [amp x meter-squared (Am^2)] is based on measurements of the magnetic induction field $\boldsymbol{B}(\boldsymbol{r}, \boldsymbol{M})$ [Tesla, T], that emanates from the target. In accordance with classical electromagnetic theory, at a distance "r" from a magnetically polarized object (e.g., ferrous UXO) if r is greater than about two times the object's largest dimension the $\boldsymbol{B}$-field that emanates from the object is given by the magnetostatic dipole approximation [9]:

$$\boldsymbol{B}(\boldsymbol{r}, \boldsymbol{M}) = (\mu/4\pi)[3(\boldsymbol{M}\bullet\boldsymbol{r})\boldsymbol{r}/r^5 - \boldsymbol{M}/r^3] \qquad \text{Eq. 1}$$

Where μ is the magnetic permeability of the surrounding media (typically $\approx 4\pi \times 10^{-7}$ Tm/A for non-magnetic media).

In principle, measurements of an object's magnetic anomaly field $\boldsymbol{B}$ can be processed in accordance with the dipole equation (or its spatial gradients) to determine the object's location $\boldsymbol{r}$ and its magnetic dipole signature $\boldsymbol{M}$. With regard to the use of a magnetic sensor system for classification of magnetic targets:

- The magnitude and direction of a target's magnetic signature $\boldsymbol{M}$ depend on the orientation of the target's ferrous materials with respect to the Earth's field and also on the size, geometry and magnetic permeability of the ferrous materials [10].
- Measurements of the magnetic signatures of underwater and buried ferrous objects can be used to classify the objects as UXO-like or clutter-like [11].

Thus, magnetic sensor systems can perform DLC of magnetic objects by i) detecting the presence of their magnetic anomaly fields, ii) processing the field variables (or, their gradients) to determine the object's location and magnetic dipole signature and iii) classifying the objects by comparing the measured dipole signatures with a previously determined list tabulating signature parameters versus previously measured/characterized signatures from known UXO. Within the scope of prototype sensor development of MM-1511, "classification" has been used in a limited sense to signify the process of accurate measurement of the 3-D Cartesian (XYZ) components of $\boldsymbol{M}$.

The magnetic field of Earth ($\boldsymbol{B}_E$) makes it difficult to use a mobile sensing platform to directly measure the 3-D vector components of $\boldsymbol{B}$. Relative to the relatively large and constant magnetic field of Earth ($\boldsymbol{B}_E$), the $\boldsymbol{B}$ field that emanates from ferrous UXO constitutes a local magnetic anomaly whose amplitude drops off as the inverse cube of the distance r from the target. Thus at distances of only a few meters from medium sized UXO (e.g., with $M \sim 10$ Am^2 and largest dimension ≤ 1 m) in accordance with Eq. 1, $B \leq 1$ nT. Spatially, over short distances (i.e., hundreds of meters) the Earth's field has a fairly constant magnitude of about 50, 000 nT; thus typically $B_E >> B$. Furthermore, the components of Earth's field can change unpredictably by tens or even hundreds of nT within tens of minutes. Thus, direct measurements of $\boldsymbol{B}$ must somehow take into account the temporal variations of $\boldsymbol{B}_E$. This is not easy to do from a moving platform because as the platform changes its orientation its vector field sensing elements are measuring

components of a total field ($\boldsymbol{B}_T$) where $\boldsymbol{B}_\mathbf{T} = \boldsymbol{B}_\mathbf{E} + \boldsymbol{B}$. Consequently, as a mobile sensor system turns in the Earth's field its field sensing elements will see non-target-related field changes equal to $B_E$cosine(θ) where θ is the angle between $\boldsymbol{B}_E$ and a vector magnetometer's field-sensing direction. Thus, as a mobile vector magnetometer rotates in general unconstrained motion, it can measure sensor-orientation-dependent, non-target-related changes in field components with amplitudes between +/- 50,000 nT. The platform orientation dependent changes constitute a type of platform motion noise that impede direct measurements of components field; therefore, mobile point-by-point DLC of magnetic targets generally requires the use of magnetic gradient sensors (i.e., tensor gradiometers) that measure the gradient of $\boldsymbol{B}$- field.

The Earth's main field B_E has a small (~0.02 nT/m) gradient [12]. Therefore, accurate determination of the location $\boldsymbol{r}$ and magnetic signature $\boldsymbol{M}$ of magnetic targets from mobile sensing platforms generally involves the use of tensor gradiometer-type sensors that greatly reduce B_E–related platform motion noise by measuring B-field gradients between multiple sensors. A magnetic gradiometer measures $\nabla(\boldsymbol{B}_\mathbf{T}) = \nabla(\boldsymbol{B}_\mathbf{E} + \boldsymbol{B}) \approx \nabla\boldsymbol{B}$. The first order magnetic ($\boldsymbol{G}$) of the magnetic anomaly field i.e., $\boldsymbol{G} = \nabla\boldsymbol{B}$ is a second-rank tensor with nine matrix elements (G_{ij} where subindices i, j represent Cartesian XYZ components and δ_{ij} is the Kronecker delta $\delta_{ij} = 1$ for i =j, $\delta_{ij} = 0$ for i ≠ j). The G_{ij} are given by:

$$G_{ij} \equiv (\nabla\boldsymbol{B})_{ij} \equiv \partial B_i/\partial r_j = -3\,(\mu/4\pi)\,[\boldsymbol{M}\bullet\boldsymbol{r}(5r_i r_j - r^2\delta_{ij}) - r^2(r_i M_j + r_j M_i)]\, r^{-7} \qquad \text{Eq. 2a.}$$

and the $\boldsymbol{G}$ tensor is represented in matrix form by;

$$\boldsymbol{G} \equiv \begin{matrix} G_{xx} & G_{xy} & G_{xz} \\ G_{yx} & G_{yy} & G_{yz} \\ G_{zx} & G_{zy} & G_{zz} \end{matrix} = \begin{matrix} \partial B_x/\partial x & \partial B_x/\partial y & \partial B_x/\partial z \\ \partial B_y/\partial x & \partial B_y/\partial y & \partial B_y/\partial z \\ \partial B_z/\partial x & \partial B_z/\partial y & \partial B_z/\partial z \end{matrix} \approx \begin{matrix} \Delta B_x/\Delta x & \Delta B_x/\Delta y & \Delta B_x/\Delta z \\ \Delta B_y/\Delta x & \Delta B_y/\Delta y & \Delta B_y/\Delta z \\ \Delta B_z/\Delta x & \Delta B_z/\Delta y & \Delta B_z/\Delta z \end{matrix} \qquad \text{Eq. 2b.}$$

The finite difference elements, $\Delta B_x/\Delta x$, $\Delta B_x/\Delta y$, $\Delta B_x/\Delta z$, etc, represent the fact that in practice, a tensor gradiometer determines first-order magnetic gradient components by measuring B_T -field components at separate points of a sensor array, subtracting the field values at one point from field values at another point (thereby subtracting out the common-mode B_E components) and dividing the resulting differential magnetic anomaly field values by the distances Δx, Δy, Δz between the points. As a result of Maxwell's Equations for divergence and curl of $\boldsymbol{B}$ for locally source-free, static anomaly fields (i.e., $\nabla\bullet\boldsymbol{B} = 0$ and $\nabla \times \boldsymbol{B} = 0$) the gradient tensor matrix is "traceless" and "symmetric" and so measurement of just five independent tensor components is sufficient to determine the full, nine component gradient tensor.

Expansion of Eq. 2a in terms of its components results in a set of five independent equations that relate measured gradient components coupled to six unknown quantities-namely, three components of target location $\boldsymbol{r}$ (i.e., x,y,z) and three components of magnetic dipole signature (i.e., M_X, M_Y, M_Z) magnetic dipole moment variables.

Thus:

$$\partial B_x/\partial x = (\mu/4\pi)\,[3x(3r^2 - 5x^2)M_x + 3y(r^2 - 5x^2)M_y + 3z(r^2 - 5x^2)M_z\,]r^{-7} \qquad \text{Eq.2c}$$
$$\partial B_y/\partial y = (\mu/4\pi)\,[3x(r^2 - 5y^2)M_x + 3y(3r^2 - 5y^2)M_y + 3z(r^2 - 5y^2)M_z\,]r^{-7}$$
$$\partial B_z/\partial z = (\mu/4\pi)\,[3x(r^2 - 5z^2)M_x + 3y(r^2 - 5z^2)M_y + 3z(3r^2 - 5z^2)M_z\,]r^{-7}$$
$$\partial B_z/\partial z = -(\partial B_x/\partial x + \partial B_y/\partial y)$$

$$\partial B_x/\partial y = (\mu/4\pi)\,[3y(r^2 - 5x^2)M_x + 3x(r^2 - 5y^2)M_y - 15xyzM_z\,]r^{-7} = \partial B_y/\partial x$$
$$\partial B_x/\partial z = (\mu/4\pi)\,[3z(r^2 - 5x^2)M_x - 15xyzM_y + 3x(r^2 - 5z^2)M_z]r^{-7} = \partial B_z/\partial x$$
$$\partial B_y/\partial z = (\mu/4\pi)\,[-15xyzM_x + 3z(r^2 - 5y^2)M_y + 3y(r^2 - 5z^2)M_z]r^{-7} = \partial B_z/\partial y$$

The equations 2c are nonlinear functions of position and linear functions of dipole moment. Prior approaches to determination of ***r*** and ***M*** include inversion of (2.3a) and a dipole equation-based iterative least-squares-fit to the tensor equations (2,3a) [2]. These approaches are computationally intensive and can contain ambiguous results (multiple solutions for target position, etc.) unless that either a) time series of 5-gradient-component data sets are taken at accurately known sensor locations (and orientations) or b) a 5-gradient set and at least one additional independent variable relating ***r*** and ***M*** (e.g., a vector component of ***B***) simultaneously can be measured at a single point in space. Essentially, conventional tensor gradiometry has two major intrinsic problems that do not allow it to perform true real time point by point localization and classification of magnetic targets; namely:

1. Five independent equations are insufficient to perform true real-time, point-by-point determination of all six components of ***r*** and ***M***.
2. Magnetic gradient tensor components are themselves sensitive functions of sensor platform orientation and, therefore, are susceptible to platform orientation dependent motion noise.

In practice, problems 1 and 2 have impeded the practical application of conventional tensor gradiometry to man-portable and/or other highly mobile sensing platforms. The magnetic STAR concept was created to solve problems 1 and 2 and thereby provide a magnetic sensing technology capable of true point by point with no constraints on sensor platform motion.

The following paragraphs highlight details of the Magnetic Scalar Triangulation and Ranging (STAR) concept [3, 6-8]. The scalar magnitude (or Frobenius norm) of the magnetic gradient tensor ***G*** is given by the positive square root of the trace of the product $\boldsymbol{G}\bullet\boldsymbol{G}^{\mathbf{t}}$ where "t" indicates the transpose of the matrix. In Cartesian coordinates, the trace or "contraction" (C_T^2) of $\boldsymbol{G}\bullet\boldsymbol{G}^{\mathbf{t}}$ can be represented by the following expression.

$$C_T^2 = \Sigma\,(G_{ij})^2 = (\partial B_x/\partial x)^2 + (\partial B_x/\partial y)^2 + (\partial B_x/\partial z)^2 + (\partial B_y/\partial x)^2 + (\partial B_y/\partial y)^2 + (\partial B_y/\partial z)^2 + (\partial B_z/\partial x)^2 + (\partial B_z/\partial y)^2 + (\partial B_z/\partial z)^2 \qquad \text{Eq. 3}$$

The C_T-parameters have very desirable properties for DLC of magnetic targets.

- In accordance with tensor theory, the C_T parameter are rotationally invariant scalars that are invariant under rotations of the sensor platform and thus the C_T's are intrinsically resistant to sensor platform motion noise.

- In accordance with magnetics theory (i.e., the dipole equation (Eq. 1)) the C_T are robust quantities whose relative values are monotonic central potential-like functions of sensor-target distance.

These properties are exploited in the Magnetic Scalar Triangulation and Ranging (STAR) method for localization/classification of magnetic objects. The properties of C_T that enable the STAR approach can be explicitly represented by combining Eq. 2c and Eq. 3. Then, the relation between magnitudes of C_T, r and M can be reduced to a form analogous to that of a central-potential-type function; namely:

$$C_T = k(\mu/4\pi)M/r^4 \qquad \text{Eq. 4}$$

where "k" is an "asphericity" parameter, a number that characterizes the departure of the C_T field from perfect spherical symmetry. Asphericity parameter k slowly varies from about 7.2 for points in space that that are aligned with the target's dipole axis to 4.2 for points transverse to the dipole axis. Fig. 2 is a graphical representation of the geometrical relations between the C_T fields and a magnetic dipole target. The k-parameter will be essentially constant over the volume of a sensor system when $r > 3$ times the distances between C_T-measurement points in the sensor system. In accordance with Eq. 4, if $k \approx$ constant, then different values of C_T–scalars to a good approximation are a result only of different r-distances between the target and the respective measurement points.

The basic MagSTAR process is illustrated by the following simple example. A MagSTAR sensor measures parameters C_{T1} and C_{T2} simultaneously at two points 1 and 2 within the sensor system. Points 1 & 2 are at distances r_1 and r_2 (and $r_2 = r_1 + \Delta r$) from a magnetic object with dipole moment M, then target location r relative to the MagSTAR sensor's position can be triangulated by:

$$C_{T1} = k(\mu/4\pi)M/r_1^4 \;;\; C_{T2} = k(\mu/4\pi)M/r_2^4 \;\rightarrow\; C_{T1}/C_{T2} = (r_2/r_1)^4 \rightarrow r_2 = r_1(C_{T1}/C_{T2})^{0.25}$$

and so $r_1 + \Delta r = r_1(C_{T1}/C_{T2})^{0.25} \rightarrow r_1 = \Delta r\,[(C_{T1}/C_{T2})^{0.25} - 1]^{-1}$ Eq. 5.

Eq. 5 represents the result from a simplified version of the STAR triangulation process. Simple refinements of the process allow calculation of the Cartesian components of $\boldsymbol{r}$. Then substitution of the r-components into any three of equations 2c will yield an immediately solvable set of three linear equations the three Cartesian components (M_X, M_Y, M_Z) of magnetic dipole signature $\boldsymbol{M}$. Thus the STAR process allows point-by-point (i.e., at every position/orientation of the sensor system) determination of the vector components of a magnetic object's location $\boldsymbol{r}$ and magnetic dipole signature $\boldsymbol{M}$. The values of r_X, r_Y, r_Z and M_X, M_Y, M_Z determined by the basic STAR process provide a close approximation to the true values; however, they are subject to "asphericity errors" due to the aspherical nature of contours of tensor magnitude C_T [6]. For improved DLC accuracy the basic STAR-derived location and classification parameters can be used as initial parameters in a least squares fit (LSF) process that will rapidly converge to the true values of $\boldsymbol{r}$ and $\boldsymbol{M}$ [13,14]. Fig. 3 summarizes the mathematical and geometrical bases of the MagSTAR concept for point-by-point, motion noise resistant DLC of isolated magnetic targets. while Fig. 4 represents a potential STAR-based solution of the difficult multi-target DLC problem.

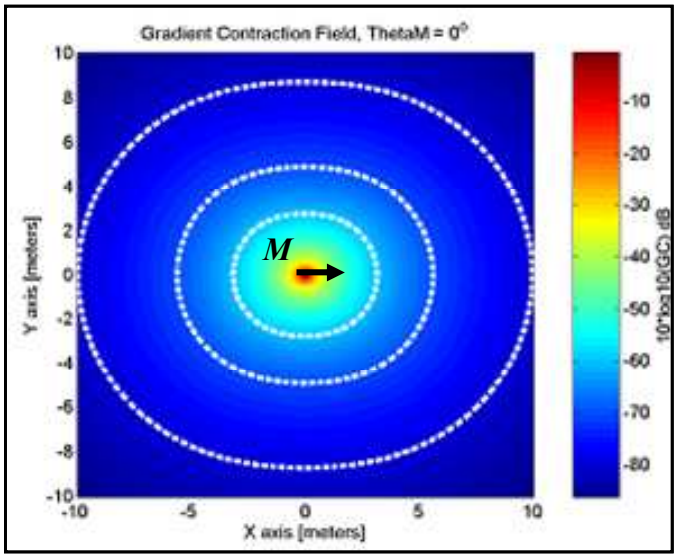

Fig. 2. Two-dimensional theoretical representation of the C_T field from a magnetic dipole target (→) with a magnetic dipole moment M = 14.5 Am^2. Contours of $C_T = [\Sigma\ (G_{ij})^2]^{0..5} = k(\mu/4\pi)\ Mr^{-4}$ = constant form concentric spheroidal "equipotential surfaces" centered on the target location. The dashed white lines highlight a few C_T contours at 10dB intervals,

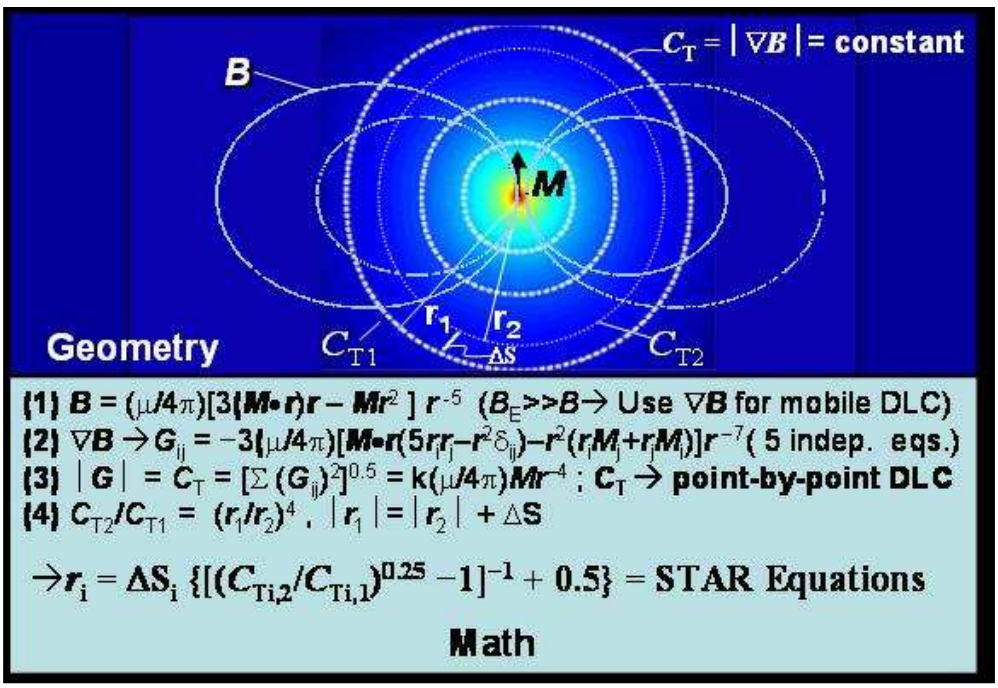

FIG. 3. Summary of Magnetic Scalar Triangulation and Ranging (MagSTAR) concept.

- Magnetic UXO with dipole moment $\boldsymbol{M}$ produces a magnetic anomaly field $\boldsymbol{B}$. A 3-D STAR Sensor (Fig. 5) measures a target's magnetic field $\boldsymbol{B}(\boldsymbol{r})$ at multiple points simultaneously.
- A system processor calculates magnetic gradient tensors ($\boldsymbol{G}_i = \nabla_i\ \boldsymbol{B}$) and the tensors' magnitudes (or "contractions" $C_{T,\,I} = \{[\Sigma\ (G_{ij})^2]^{0.5}\}_I = k(\mu/4\pi)M\ r_I^{\ -4}$ at six spatially separate points (I) where (as shown in Fig. 5) I = +X, -X, +Y, -Y, +Z, -Z within the sensor array.
- The STAR Algorithm uses ratios of C_T-parameters to triangulate target location vector $\boldsymbol{r}$, then the XYZ components of $\boldsymbol{r}$ are used in Eq. 2c to calculate the magnetic dipole vector $\boldsymbol{M}$.

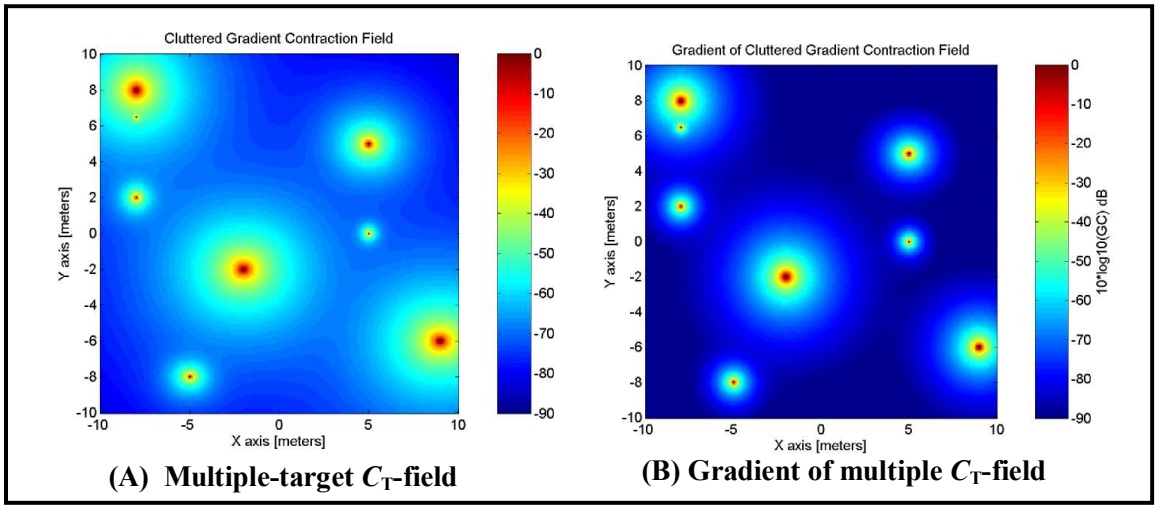

Fig. 4. Theoretical representations of moderately cluttered gradient contraction field distribution from multiple targets. **(A)** Multiple-target, cluttered C_T –field from eight UXO-type targets including 1000 lb, 500 lb and 250 lb bombs; oil drum; two 81 mm shells and two 60 mm shells. "Saddle points" in the C_T-field result where there is significant overlap between target fields. At saddle points the dipole approximation is not valid and the simple C_T-based STAR process is inaccurate.
(B) A solution for moderate clutter densities. Taking the gradient of the high clutter density C_T field will reduce the effect of potential field saddle-points between clustered targets. The resulting ∇C_T vector will point close to the direction of the nearest and/or strongest target. The cubic symmetry of the prototype STAR Sensor facilitates development of multiple channels of symmetrically disposed ∇C_T and ∇G_{ij} data that can be used to discriminate UXO embedded in clutter.

In order to use the C_T scalars to measure the six vector components of target position $\boldsymbol{r}$ and magnetic dipole moment $\boldsymbol{M}$, a STAR gradiometer should be capable of simultaneous measurement of a 3-dimensional (3-D) set of six C_T parameters. Fig. 5 shows a preferred geometry for a STAR gradiometer: A cubic array of Triaxial Fluxgate Magnetometers (TFM). Magnetic field data from the TFMs are combined by a processor (indicated in the block diagram of Fig. 6) in such a way that each face of the cube corresponds to an individual tensor gradiometer. Then, the data from the TFMs in each face of the cube determine a C_T parameter and the C_T parameters from the six faces of the cube form an 3-D array with a set of two parameters along each of the sensor system's Cartesian XYZ coordinate axes. The STAR Algorithm uses ratios of the two-parameter sets of gradient tensor magnitudes C_T (also known as gradient contractions) to triangulate and calculate the X,Y,Z components of target position. For example, (with reference to Fig. 7) the Z-component of target position (with respect to the center of the cubic array) is:

$$r_Z = \Delta S_Z \{[(C_{T,+Z} / C_{T,-Z})^{0.25} - 1]^{-1} + 0.5\}$$

where $C_{T,+Z}$ and $C_{T,-Z}$ are $C_{T,I}$ -parameters located, respectively, in the cube faces at $+ 0.5\Delta S_{+Z,-Z}$ and $-0.5\Delta S_{+Z,-Z}$, and ΔS_Z is the projection in the $\boldsymbol{r}$-direction of the Z-direction triangulation baseline (i.e., distance between $C_{T,+Z}$ and $C_{T,-Z}$) [3, 6,7].

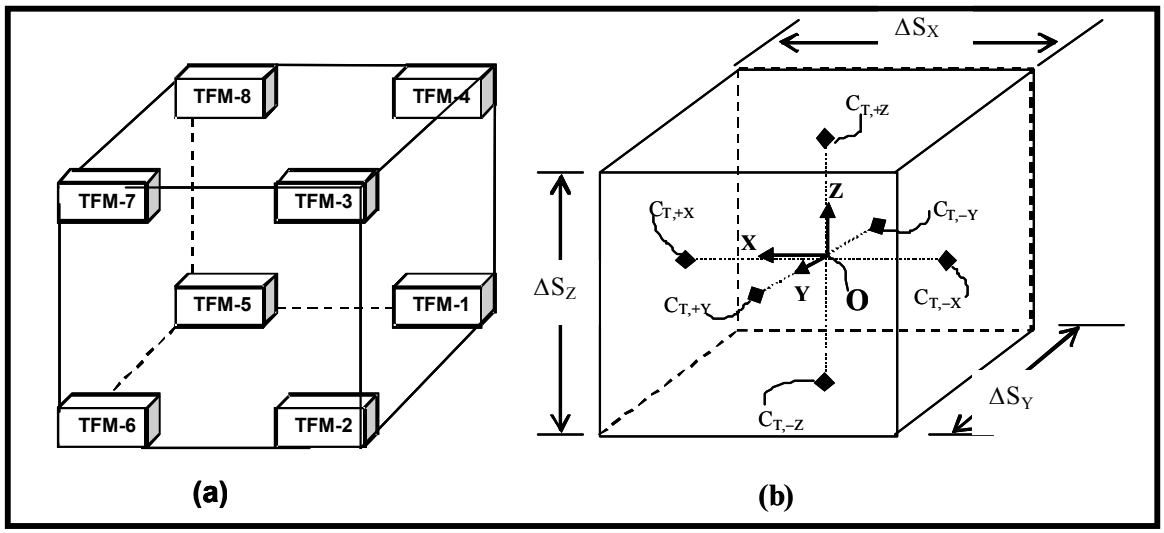

Fig. 5. Preferred geometry for a MagSTAR-type sensor array: a "STAR Cube" [8].
(a) A cubic array of 8 Triaxial Fluxgate Magnetometers (TFM-1 –TFM-8) measures 8 sets of XYZ components of ***B***-field. Data from the TFMs are combined to produce six spatially separate gradient tensors $\boldsymbol{G}_{\mathbf{I}}$ (one for each face of the cubic array) and their respective $C_{T,\,I}$ parameters.
(b) Geometrical relation between $C_{T,\,I}$ parameters ($C_{T,\,+X}$, $C_{T,\,-X}$, $C_{T,\,+Y}$, $C_{T,\,-Y}$, $C_{T,\,+Z}$, $C_{T,\,-Z}$), triangulation baselines (ΔS_X, ΔS_Y, ΔS_Z) and the STAR Cube's XYZ coordinate system. For clarity of illustration, the TFM sensors at the corners of the cube are not shown.

Again, target dipole moment components M_X, M_Y and M_Z are very easily calculated by using the components r_X, r_Y and r_Z in the gradient tensor equations, Eq. (2).

Fig. 6 is a top-level sketch of the basic hardware/software configuration for Project MM-1511's prototype man-portable MagSTAR sensor.

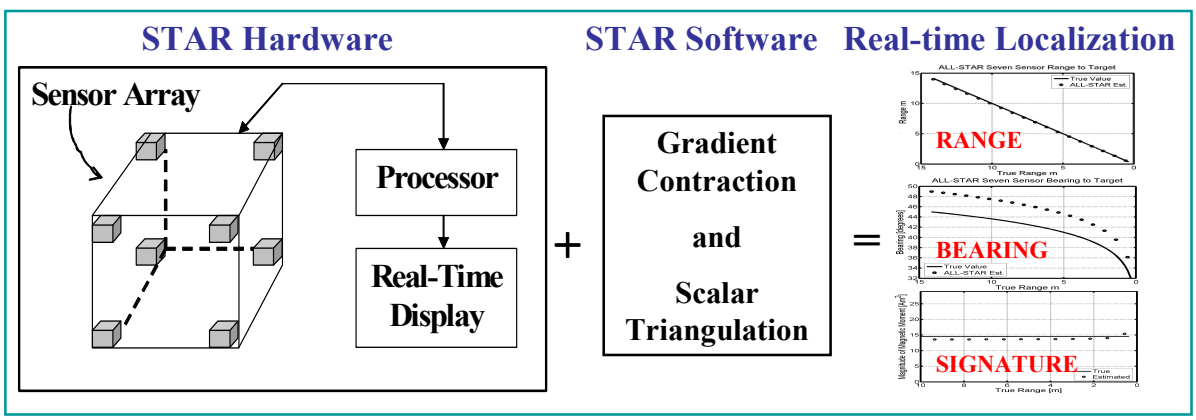

Fig. 6. Basic design and operation of a STAR Sensor. The sensor system includes:

- Hardware: Cubic array (shaded boxes) of eight low noise TFM's develops 24 channels of vector field data.
- Processor (hardware & software) develops motion-compensated tensor and scalar data and runs STAR algorithm to calculate target range ***r***, and magnetic signature ***M***. Here the term gradient contraction is synonymous with gradient tensor magnitude C_T.
- Display unit provides point-by-point real-time display of target-parameters ***r*** and ***M***.

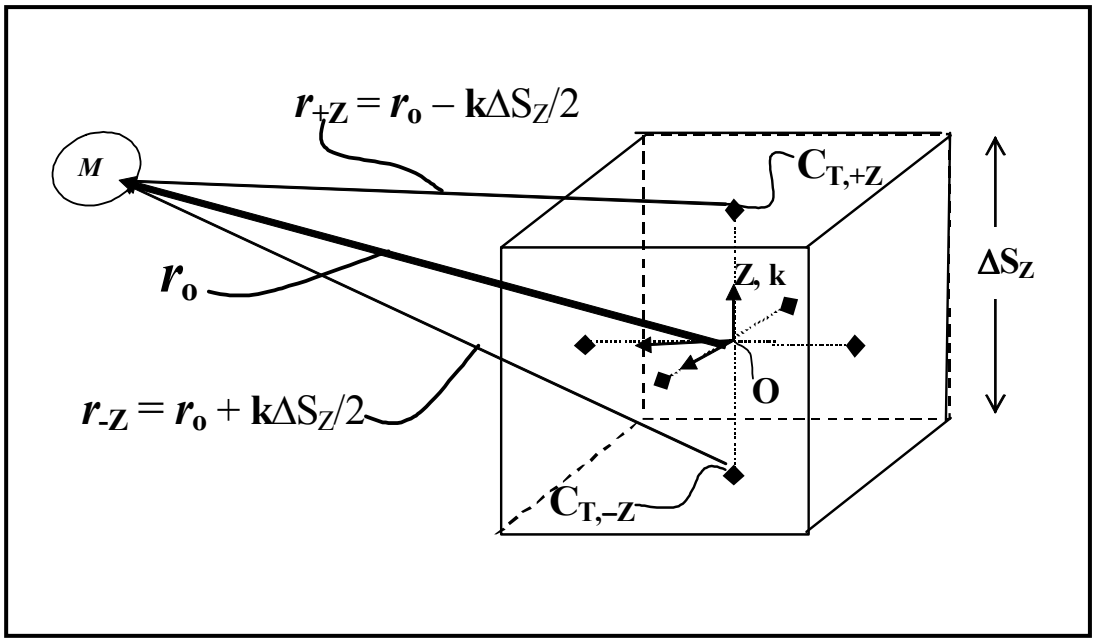

FIG. 7. Relation between the sensor-target vector $\boldsymbol{r}_o$ (relative to the center of the STAR cube), vectors $\boldsymbol{r}_{+Z}$ and $\boldsymbol{r}_{-Z}$ from $C_{T,+Z}$ and $C_{T,-Z}$ measurement points to target (***M***) and the triangulation baseline ΔS_Z. For clarity, the $\boldsymbol{r}_i$ vectors, C_T measurement points and triangulation baselines corresponding to the X- and Y-directions are not shown.

Fig. 7 illustrates the geometrical basis for triangulation of the Z-component of target location vector $\boldsymbol{r}_o$ with respect to the center of symmetry of a STAR-cube sensor array. Similar geometrical relations are used to triangulate the X and Y components of $\boldsymbol{r}_o$. Although the triangulated components are subject to asphericity errors, they provide a very effective basis for improved algorithms (such as the directional derivative and least squares fit algorithms described in the Results section) that allow the MagSTAR to perform very accurate DLC for any orientation or state of motion of the sensor platform with respect to the target.

Prior R&D on the STAR concept.

At NSWC PCD, verification of the basic STAR concepts of robustness and rotational invariance have been accomplished through numerous field tests of simple gradiometers [4,5,7,8] and modeling and simulation [5-7]. The initial STAR concept was created in FY 2001 to provide a magnetic sensor system technology for small Autonomous Underwater Vehicles (AUV) such as the highly mobile crawler-type Underwater Bottom Vehicles (UBV) that were being developed for the Surf Zone Reconnaissance Project of the Office of Naval Research's (ONR) Very Shallow Water/Surf Zone Mine Countermeasures Program [4,5]. The objective of the magnetic sensor system was to detect underwater and buried mines along the sea bottom and autonomously guide the UBVs to the mines. The STAR concept was created because there did not exist any conventional magnetic sensor system technology that could function effectively onboard small, high mobility AUVs.

The initial development of the STAR approach focused on development of a two-dimensional (2-D) magnetic anomaly guidance system that would allow a UBV to "home in on" an underwater mine. As detailed in [4,5], the prototype "UBV-STAR" technology used motion-noise-resistant gradient magnitude data from a 2-D gradiometric array (Fig. 8) of three Triaxial Fluxgate Magnetometers (TFM) to determine a relative bearing to target and to provide guidance/control parameters for a UBV so that it could autonomously home in on a magnetic target. The UBV-STAR Gradiometer successfully demonstrated the use of gradient magnitudes for magnetic target detection and 2-D magnetic anomaly sensing based guidance of AUVs to buried targets. However, scalar data from a 2-D array can not provide an effective basis for real-time, point-by-point localization and classification of magnetic objects. Nevertheless, the results from the UBV STAR implied that a 3-D STAR concept could be developed to provide a uniquely effective technology for motion noise resistant, high-speed, standoff DLC of magnetic targets.

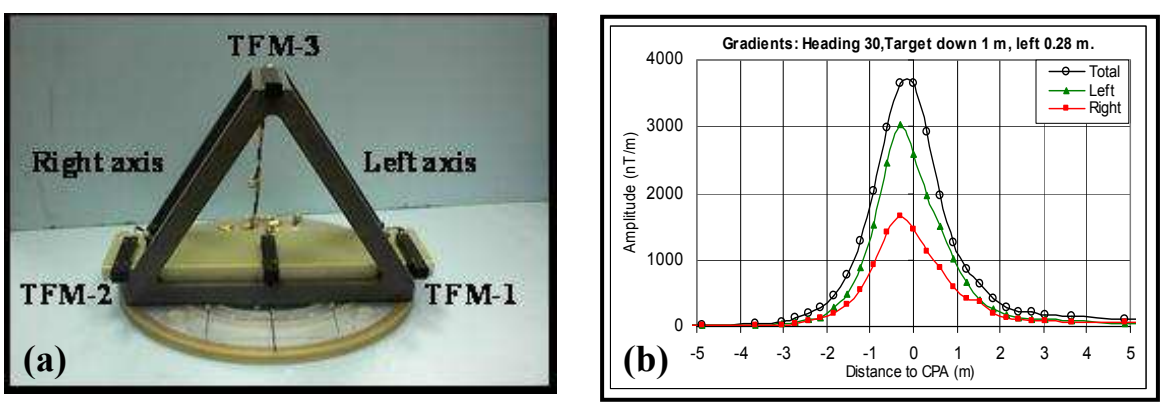

Fig. 8. Prototype 2-D "UBV-STAR" Gradiometer and data.
(a) UBV STAR gradiometer comprised by an array of TFMs (black rectangles). An "axis" of the array is comprised by a set of two TFMs.
(b) Data taken as the UBV-STAR was moved past a 14.5 Am^2 dipole target located 1-m below and 0.28 m to the left of the sensor path and heading. The Total, Left and Right curves respectively indicate the total nine-component tensor contraction (C_T) from TFMs 1,2&3, and partial (3-component) contractions for the UBV-STAR's Left axis (TFMs 1&3) and Right axis (TFMs 2&3). Since the target was to the left of the UBV STAR's heading the amplitude of the "Left" data curve > "Right" data. Relations between the *C*-parameters provide a simple uphill search type proximity-sensing modality for guidance of UBV-type vehicles to magnetic targets.

Materials and Methods

General approach for Project.

The principal scientific question to be investigated was the feasibility of applying the theoretical magnetic STAR concept to a man-portable sensor technology for DLC of magnetic targets. Consequently, the project's specific technical goal was to develop and demonstrate a practical and effective man-portable MagSTAR-based sensor for near-real, point-by-point DLC of magnetic UXO. Heretofore, no examples of MagSTAR technology existed; therefore, the project had to develop/adapt the materials and methods for the new man-portable sensor technology. The project's general approach has been to:

a) Design and construct a prototype man-portable magnetic STAR-type sensing system. (Year 1, 2006)

b) Experimentally demonstrate that the prototype STAR sensor, while in non uniform motion (i.e., while being hand-carried by a single individual), would perform real-time, point-by-point detection, localization and classification of magnetic targets (Year 1 and 2, 2006 and 2007).

c) Optimize the prototype sensor system for DLC of single, isolated UXO-type targets (Years 2 and 3, 2007-2008).

d) Develop an enhanced STAR Technology for DLC of UXO embedded in magnetically complex environments characterized by multiple targets, magnetic clutter and geologic noise (Year 3, 2008).

The demonstration of effective STAR sensor performance while in motion constituted the criterion for success for the project in Year 1 and the primary basis for the Go/No-Go decision for continuation of the project to Year 2. This demonstration was successfully performed early in January 2007. Achievement of the technical objectives of SERDP's MagSTAR project critically depended on specific details of the unique materials and methods used in the development of an actual working sensor system. Therefore, this Materials and Methods section presents essential details of the design and construction of the world's first prototype man-portable STAR Sensor for standoff DLC of magnetic targets [7,8].

Technical Challenges. The original design goal for gradient sensitivity of the prototype man-portable sensor system was 0.2 nT/√Hz or better at 1 Hz. This level of sensitivity would allow detection ranges on the order of 10-m for medium-large size UXO (i.e., unexploded bombs with M ~10-20 Am^2). In order to achieve this level of sensitivity for a fluxgate-based gradiometer required a well focused hardware and software development effort that would meet the following technical challenges:

- The effects of all sources of noise, that can degrade sensor system performance must be minimized. In particular, gradient imbalance errors due to electrical and mechanical misalignments of the sensors and magnetic self signature must be reduced to well under 0.2 nT.
- Effective real time discrimination of sub-nT target signatures that are embedded in the 50,000 nT Earth field (B_E) requires a unique data acquisition/signal processing system with (140 dB dynamic range) that can simultaneously discriminate multiple channels of pT-level analog signals.

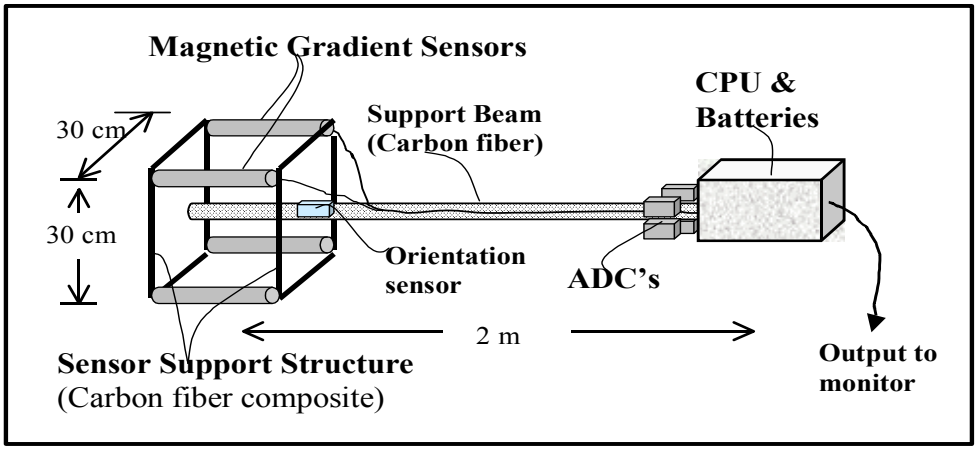

FIG. 9. Sketch of portable STAR Sensor design. (Not to scale.) A cubic array of four magnetic gradient sensors (each comprised by two Triaxial Fluxgate Magnetometers–TFM)) is mounted on a carbon-fiber support structure. Analog to digital converters (ADC) digitize the gradient sensor's analog data and a central processing unit (CPU) comprised by a single board computer processes *B*-field data and runs the STAR algorithm to provide a near real-time display of target DLC parameters to the operator's heads-up display monitor Fig. 10 (C).

- Interactive software is required to be developed for: 1) Near real-time control of data acquisition. 2) Signal processing. 3) Adaptive compensation of residual gradient channel imbalances. 4) Development and storage of target DLC parameters (e.g., range, bearing, elevation and magnetic dipole signature). 5) Real-time display of DLC parameters. 6) Input/output control of sensor system operation.
- The sensor system must be self-contained and sufficiently compact and lightweight so that it can easily be carried and operated by a single individual.

A. Hardware.

The prototype MagSTAR sensor's basic hardware configuration is sketched in Fig. 9. The hardware development involved a combination of acquisition, construction and integration of:

1. A cubic array of four Model Grad-03-300L magnetic gradient sensors by Bartington Instruments. Each Grad-03-300L (Fig. 10A) sensor contains two low noise (<20 pT (root mean square)/√Hz at 1 Hz) triaxial fluxgate magnetometers (TFM) with their respective XYZ field sensing elements separated by 30 cm. Each TFM measures XYZ components of magnetic induction field (B_X, B_Y, B_Z).
2. A precision Sensor Support Structure (SSS-Fig. 11) for mounting the Grad-03 sensors was designed and fabricated (using carbon fiber composites) at NSWC PCD.
3. A set of four Model PS6-24 24-bit digitizers (Fig. 10B) manufactured by Earth Data Ltd (http://www.earthdata.co.uk/ps6-24sp.html) provides near-simultaneous analog to digital conversion of the 24 channels of analog *B*-field data. The digitizers can be locked to a Global Positioning System (GPS) receiver to provide; a) Precise sensor system timing, and b) Tracking of the portable gradiometer's position. The digitizers' 140-150 dB dynamic range (for sample rates from 10 to 100 samples per second) allows discrimination of pT-level *B*-fields.

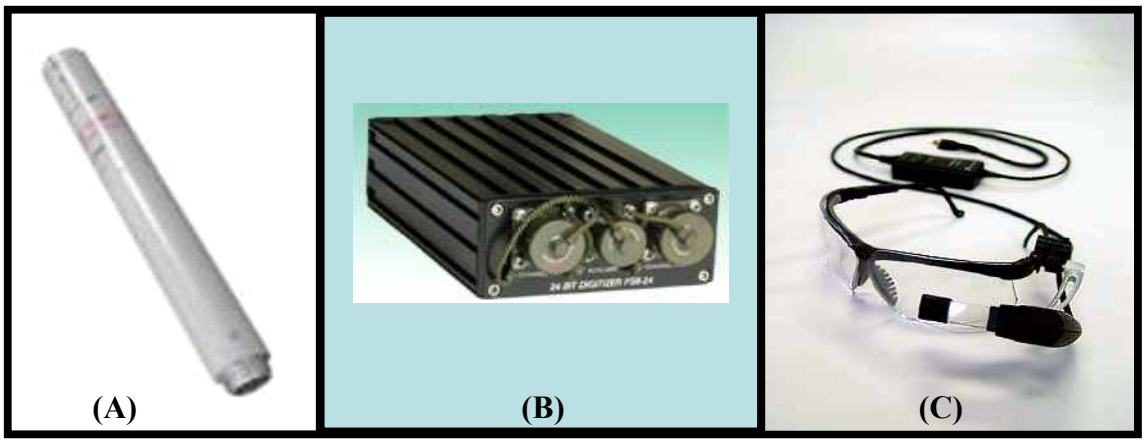

Fig. 10. Important hardware elements of the prototype MagSTAR Sensor.
(A) Gradient sensors (one shown here): An array of 4 magnetic gradient sensors of the type shown in the figure (each containing 2 Triaxial Fluxgate Magnetometers (TFM)) measures XYZ components of the magnetic anomaly field (***B***) of UXO.
(B) Data acquisition: A 24-channel data acquisition and signal processing system with integrated GPS develops, displays and stores real-time magnetic target DLC data. Principal elements of the system are four six-channel, 24-bit ADC (one shown here) and a Single Board Computer (SBC) visible in Fig. 11.
(C) Operator's Display Unit: A heads-up display unit that weighs about 2 ounces clips onto the operator's safety glasses and provides a real time indication of target DLC data.

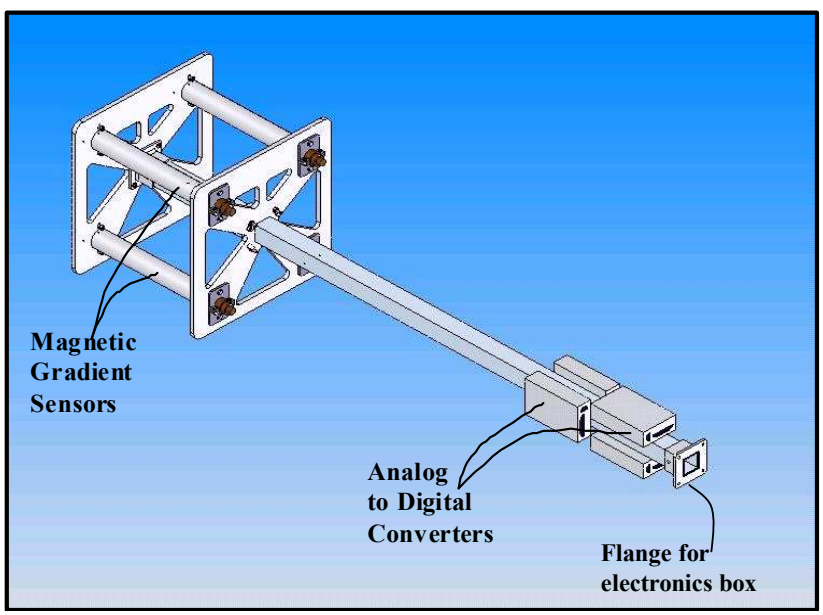

Fig. 11 Drawing of sensor support structure (SSS). The SSS (visible in Figs. 16, 20 and 21) was very carefully designed and constructed using carbon-fiber composite materials to perform the critical function of maintaining the respective XYZ *B*-field sensing axes of the magnetic gradient sensors. Ideally, the TFMs should be rigidly aligned in parallel to within 0.001° to minimize motion noise due to acceleration-dependent changes in mechanical alignment during operation of the hand-carried sensor.

4. A MicroStrain Inc. Model 3DM-GX1 orientation sensor (Fig. 13) comprised by a triaxial magnetometer, triaxial accelerometer and a triaxial rate gyro provides a reference frame for: a) Compensation of residual gradient imbalance errors, b) Indication of sensor system orientation in earth-frame coordinates.
5. A Single-Board Computer/CPU (SBC): a) Stores *B*-field, GPS and orientation data. b) Runs the imbalance compensation algorithm. c) Runs the STAR algorithm to develop the target's DLC parameters. d) Outputs the DLC parameters to the operator's monitor and input/output (I/O) device. Initially (in 2006-2008) Pentium III-based SBC's by AMPRO, Inc.(visible in Fig. 12A) and WinSystems were used in the MagSTAR sensor; however, these SBCs (especially the WinSystems) were trouble-prone and rather slow. In late 2008 the SBC was upgraded to a much more powerful, fast and reliable dual-core processor (IEI Model NANO 9452 with Intel Core-Duo microprocessor) capable of running advanced signal processing algorithms for discrimination of UXO in magnetically cluttered areas.
6. For the MagSTAR with AMPRO SBC, lithium-polymer batteries provide electrical power for the gradient sensors, digitizers and SBC. The entire battery set weighs 0.7 kg and will allow a safe operating time of three hours for the STAR Gradiometer. For the NANO-9452 SBC, a single lithium-polymer battery weighing 0.9 kg feeding a multi-voltage, regulated power supply provide about 2.5 hours operating time for the entire system including field-sensors, digitizers, SBC and the orientation sensor.

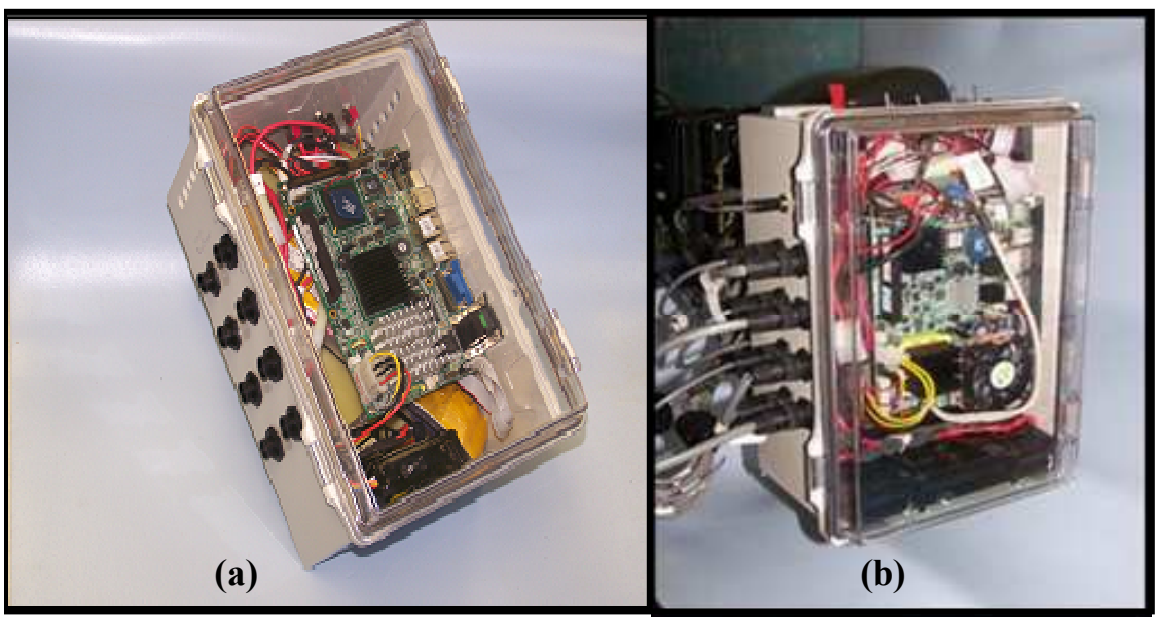

Fig. 12. The STAR Sensor's signal processing and control unit (the electronics box). (a) Original unit with AMPRO SBC visible in center of box. The original SBC was trouble-prone and not adequate for running advanced signal processing algorithms.
(b) Signal processing and control unit upgraded in 2008 with very effective dual-core IEI Inc. NANO-9452 SBC.

Each box contains a Single Board Computer (SBC), Input/Output (I/O) and control circuitry, lithium-polymer batteries and power supply circuitry. The boxes' dimensions are 14 x 17.5 x 26.5 cm (5.5 x 7 x 10.5 inches).

Fig. 13. The orientation sensor for the prototype Man-Portable STAR Sensor. The orientation sensor combines a triaxial magnetometer, triaxial accelerometer and triaxial rate gyro in a small (6.5 x 9.0 x 2.5 cm) 75-gram package.

7. Signal processing and control units (electronics boxes-Fig. 12) containing the SBC, lithium-polymer batteries, power supply and associated I/O circuitry were designed and constructed at NSWC PCD.
8. A Model SV-6 Head-Mounted Display (Fig. 10(C) by MicroOptical Inc., provides a very convenient, lightweight display of target DLC parameters for the operator. For field tests with the MagSTAR operating completely untethered (with no external cables attached) a touchpad mouse along with the head-mounted display allow the operator control over sensor operational modes. Alternately, if desired any computer display unit and keyboard also can be used to provide I/O.

B. Software.

The STAR technology combines novel hardware and signal processing approaches. Part of the sensor design process involved development of new software to provide modeling and simulation of likely performance of a proposed cubic STAR Sensor geometry. As indicated in the simplified flowchart of Fig. 14 and presented in more detail in the "super_starJO12192008." program listings in Appendix (B), the project included a very substantial software development effort. The software was written primarily in MATLAB. In 2008, the MagSTAR signal processing system was upgraded with a 64-bit dual-core SBC that required new data acquisition software to be written in C programming language. The software:

- Performs interactive data acquisition from, and control of, the STAR sensor data channels containing *B*-field , GPS orientation and temperature data.
- Processes the magnetic field vector and tensor data to provide adaptive gradient imbalance error compensation by correlating residual motion-dependent sensor imbalance errors with platform orientation to mitigate residual gradient imbalances and motion noise errors [7,8].
- Runs the 3-D Scalar Triangulation and Ranging algorithm for near real-time target localization, classification and target homing.
- Performs the more advanced signal processing functions that were developed in 2008 for eliminating asphericity errors and providing a much more accurate and effective target classification capability. These functions include the directional derivative (DD) and least squares fit (LSF) algorithms described below.
- Provides the sensor system operator with an interactive, near real-time display of target DLC parameters and sensor operational modes.

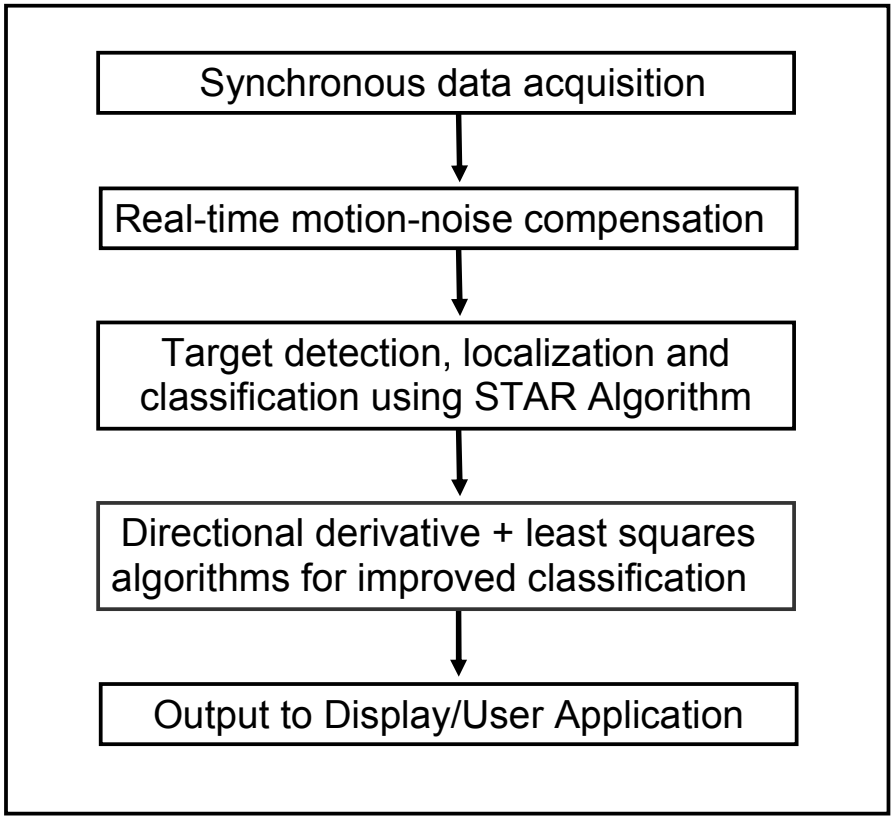

Fig. 14 Simplified flow diagram of MATLAB-coded software for prototype MagSTAR sensor. The diagram represents about 3000 lines of code (listed in Appendix (B); however, the program could be substantially reduced (by about 40%) in more optimized and faster C-based code for a next-generation sensor system.

Improved methods: Directional derivative- and least squares-based algorithms

Improved STAR methods based on "directional derivative" (DD) and least squares fit (LSF) approaches were developed in 2008 to provide more effective and accurate DLC performance [13,14]. The DD and LSF approaches also provide a basis for applying the STAR technology in magnetically cluttered regions. The DD method is based on the fact that the magnitude of the magnetic gradient tensor can be expressed as a central-potential-type scalar function; that is, $C_T = k(\mu/4\pi)Mr^{-4}$ (Eq. (4)). Consequently: (i) ∇C_T is a vector that points close to the direction of the target relative to the sensor platform. (ii) ∇C_T can be used for determining a close approximation (within asphericity error limits) to the true target-location vector $\boldsymbol{r}$ and magnetic dipole vector $\boldsymbol{M}$. Furthermore, the values for $\boldsymbol{r}$ and $\boldsymbol{M}$ obtained by the DD method can be used as initial parameters in an iterative Eq. (2)-based LSF process for: (a) More accurate localization and discrimination of UXO by eliminating the aforementioned asphericity errors. (b) Development of a more effective modality for discriminating between multiple targets. The LSF method combines a linear part for calculation of $\boldsymbol{M}$ and a non-linear part for calculation of $\boldsymbol{r}$. In particular, the linear LSF method first uses the components of $\boldsymbol{r}$ that are obtained by the DD method in the gradient tensor equations to calculate a first value for the components of the target's magnetic dipole signature $\boldsymbol{M}$ and then iteratively adjusts the $\boldsymbol{M}$-components in Eq. (2) to get a next improved fit to the measured gradient tensor components. The non-linear LSF part of the process iteratively adjusts the XYZ values of $\boldsymbol{r}$ (i.e., r_X, r_Y, r_Z) in Eq. (2) to provide another, better fit to the measured gradient tensor components. The overall LSF process cycles between the linear and non-linear parts until the best least squares fit to $\boldsymbol{r}$ and $\boldsymbol{M}$ are obtained. Since the DD algorithm by itself yields a close approximation to the true $\boldsymbol{r}$ and $\boldsymbol{M}$, two iterations of the LSF process typically will provide a reasonably good fit to measured data. Field test data from the DD/LSF algorithm are presented in the Results and Accomplishments section.

C. Sensor integration.

The sensor system's hardware and software were developed concurrently and, as indicated in Fig. 15, integrated into four functional blocks with each block comprising one Grad-03 gradient sensor, one six-channel PS6-24 Digitizer and the data acquisition and gradient imbalance compensation software corresponding to the respective sensor-digitizer set. Initially only enough hardware for one block (i.e., one-fourth of the complete MagSTAR sensor. The four blocks were designed to be functionally the same. Therefore, the data acquisition and signal processing (gradient imbalance compensation, etc.) software that was developed for the first block could very rapidly be adapted to the other blocks once the complete set of sensor system components had arrived at NSWC PCD. Hardware and software for a complete data acquisition block plus SBC block (shown in Fig. 15) were constructed and tested prior to receipt of the complete sets of all four Grad-03 sensors and PS6-24 ADC's. Thus, when all of the system's components (i.e., Grad-03 sensors, ADCs, SSS, SBC, etc.) were finally onboard at NSWC PCD (in December 2006) the final integration and test of the complete prototype MagSTAR sensor (Fig. 16) proceeded very rapidly.

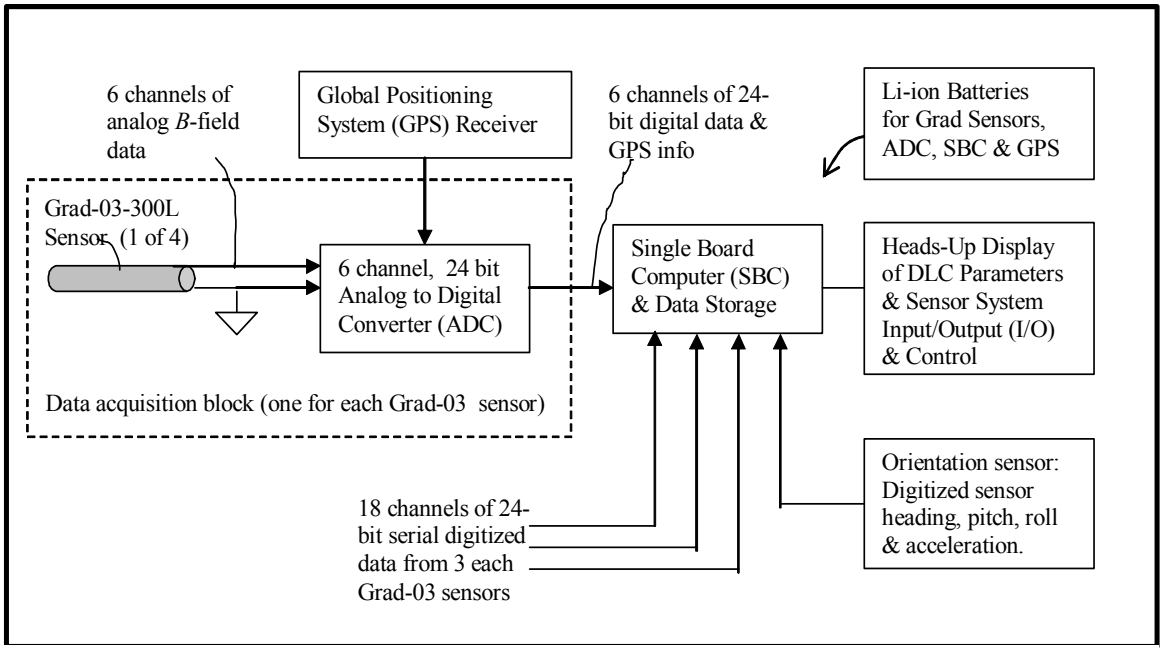

Fig. 15. Signal flow diagram for prototype STAR system. Analog *B*-field data from four Grad-03-300L sensors are digitized by four six-channel PS6-24 ADCs. The 24-channel digital data stream is processed in the SBC to generate: 1) Raw gradient data. 2) Motion compensated gradient data. 3) Gradient contraction parameters. 4) Target DLC parameters. 5) Near real-time (within three seconds) display of DLC parameters (range, bearing, elevation and magnetic signature to operator's display.

Fig. 16. The prototype Man-Portable STAR Sensor resting on a triangle with 40 cm sides (and a 1-foot wooden ruler at the top of the triangle). The prototype sensor system uses commercial "off the shelf" electronics that are rather heavy and magnetic. Consequently, the prototype sensor is heavier (its total weight is 17 kg (38 lb) including batteries) and larger (its overall length is 2.4 m (7.9 feet)) than optimal.. A next-generation "Mark II" MagSTAR sensor could use optimized electronics and be made much smaller and lighter.

D. Test and Evaluation of complete sensor.

Sensor system test and evaluation (T&E) primarily consisted of field tests performed to characterize the prototype man-portable sensor's DLC performance against isolated magnetic dipole targets and collect data for sensor optimization. The field tests included operational tests of sensor performance against isolated targets while the sensor was being hand-carried by a single individual. The primary objectives of the field tests were to:

a) Verify correct operation of the completely integrated portable STAR Sensor.
b) Demonstrate the general validity of the STAR concept.
c) Determine the STAR Sensor's capability for performing effective DLC of a magnetic UXO like target while the sensor platform is in motion.
d) Provide experimental verification for the Project's progress in Year-1. In particular, the field tests provided input for the Go/No-Go decision regarding the continuation of the project to Year-2 (2007).

E. Optimization of Sensor

The first prototypes of any new technology will generally require significant improvement and refinement before the technology becomes fully effective. Therefore, based on the results of field tests and computer simulations, improvements to the MagSTAR sensor system's hardware, software and ergonomics were ongoing throughout the duration of the project. The goal of the development/optimization effort was (within the project's programmatic constraints) to produce a truly effective and user-friendly technology that can be used to perform DLC of UXO in all environments including magnetically complex environments.

Results and Accomplishments

Project MM-1511's R&D effort focused on development, demonstration and optimization of a new man-portable magnetic sensor technology based on a heretofore untested 3-D magnetic STAR concept for point-by-point DLC of magnetic objects such as UXO. Therefore, the project's results and accomplishments reported here primarily relate to science and technology issues that were addressed in order to create the first prototype of the new man-portable magnetic sensor technology and to accurately characterize its capabilities and limitations. The magnetic dipole signature of ferrous UXO depends on the UXO's orientation in the Earth's magnetic field. Thus, in the sensor development and evaluation phase of the project, small, accurately characterized permanent magnets were used to simulate UXO. Consequently, most of the field tests described below were performed using permanent magnets (with constant magnetic dipole signatures) to simulate UXO. This procedure allowed more accurate characterization of the sensor system and avoided the procedural problems related to the handling of inert UXO at NSWC PCD. However, as indicated below, most of the sensor development effort involved theoretical and experimental characterization of the sensor's performance against the project's "standard target"- a permanent magnet with a 14.5 Am^2 dipole moment. Although this represents the magnetic signature of a fairly large UXO (about midway in size between a 250 lb and a 500 lb bomb), for a given sensitivity, the sensor detection range data corresponding to the 14.5 Am^2 can readily be scaled to estimate the range for any given UXO signature. (In accordance with Eq. 4 the detection range of a STAR sensor scales with the fourth root of target signature (M).)

Although the focus for the next-generation MagSTAR development effort clearly will be to demonstrate the technology against real UXO (albeit inert) real-world scenarios involving multiple targets and magnetic clutter, the focus of the development effort reported in the following paragraphs was to design, develop and optimize the first prototype of the MagSTAR technology.

Funding for MM-1511 started in FY06 and continued through FY08 (with final depletion of FY08 funds in April 2009). The following paragraphs summarize Results and Accomplishments per calendar year starting in 2006..

Results and accomplishments in 2006 (Year 1 of Project MM-1511).

Specific results and accomplishments for FY06 are listed below. Since no 3-D STAR sensor had ever been developed, the project's Year-1 objectives were to design, construct and demonstrate a man-portable sensor based on the STAR concept. The following list summarizes the project's results/accomplishments with regard to specific tasks and milestones and their month of completion..

- Sensor system design was completed (January 2006). For ease of construction, mechanical stability in motion and considerations of theoretical advantages for a scalar triangulation scheme a STAR sensor design based on a cubic array of triaxial fluxgate magnetometers (TFM) was selected. The process of selecting and ordering the Sensor's Bartington Model Grad-03-300L gradient sensors was completed in February 2006.
- Theoretical simulations calculations were performed (January-February 2006) to estimate the DLC performance of a cubic STAR sensor system performance for the

published levels of internal TFM sensor noise (i.e., < 20 pT/√Hz (root mean square-rms) at 1 Hz) for the Bartington Grad-03-300L magnetic gradient sensor. Results of the simulations are shown in Fig. 17 (and in more detail in [7,8]). The results indicate that for a 14.5 Am^2 target, sensor-element noise levels of 20 pT//√Hz would limit the effective DLC range of an ideal MagSTAR sensor to ≤ 8.7 meters.

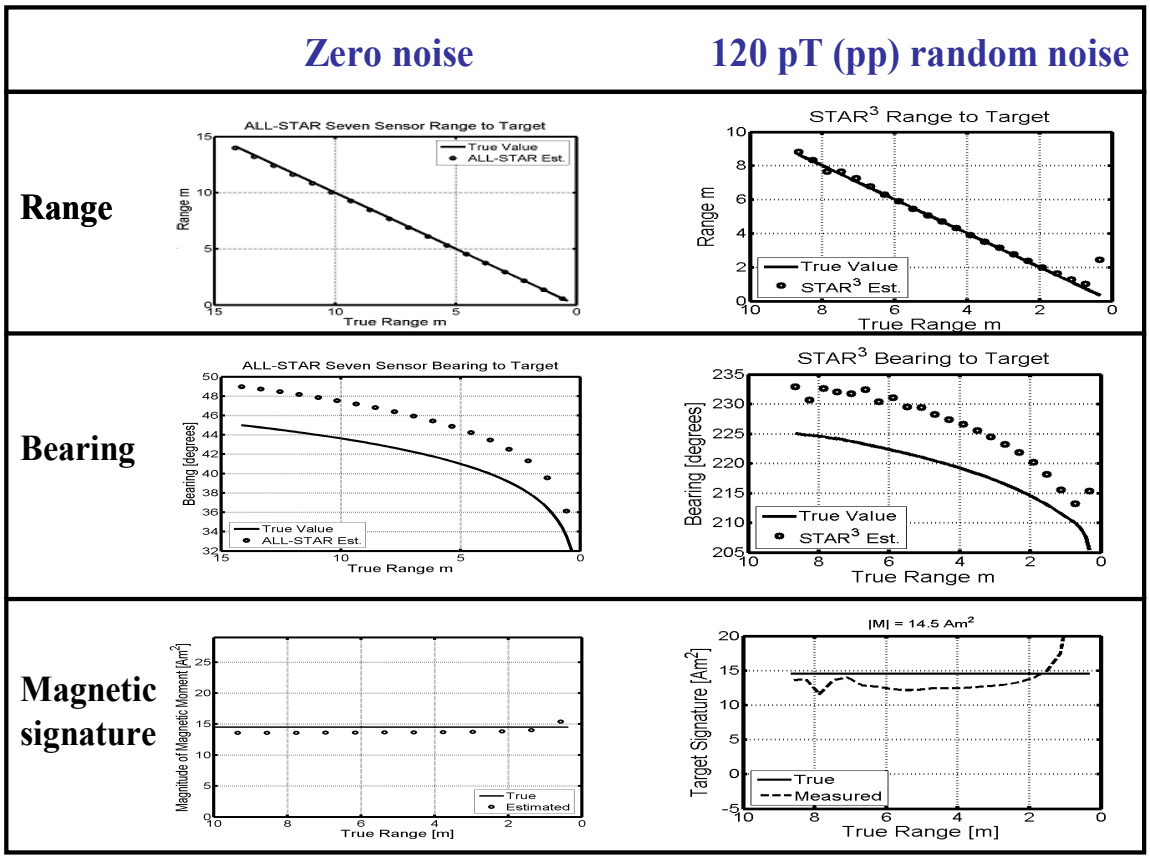

Fig. 17. Results of modeling and simulation of STAR sensor performance (results of these and other simulations are presented in more detail in [6]). The simulated range, bearing and magnetic signature data were generated (with and without internal sensor noise) by the STAR Algorithm for initial sensor positions at 45° and 225° with respect to the dipole axis of a 14.5 Am^2 target.

The data on the left represent simulations of ideal STAR sensor performance with no internal noise and, therefore, no limit on sensor DLC range.

The data on the right represent a simulation with 120 pT (pp) random noise on all TFM channels. The noise limits the STAR sensor's DLC range to 8.7 m and (between 8.7 to about 6 m) causes small dispersions from the ideal sensor measurements. However, at distances < 8.7 m, the simulated sensor performance is very robust. The variances between true and calculated values of range, bearing and magnetic moment are due to "asphericity errors" [5] that result from the aspherical nature of the contours of constant C_T shown in Figs. 2-4).

- The first of four Bartington Model Grad-03-300L magnetic gradient sensors was received at NSWC PCD in April 2006. The sensor was subjected to a series of laboratory and field tests to verify that it met published specifications with regard to noise levels in the laboratory (in the Magnetic Sensor Lab at NSWC PCD) and also functioned correctly in the field. The other three sensors of the quad-grad MagSTAR system were finally received and tested by July 2006. All four Grad-03 were tested and noise power spectral densities for several of the Grad-03's 24 field-sensing elements were measured in the NSWC PCD Magnetic Sensors Lab. The field-sensing elements noise levels were measured to be close of the manufacture's specs. For example Fig 18 indicates a noise level at 1 Hz of 17 pT/√Hz (rms) for the Y_1 field – sensing element of Grad-03-300 serial number 030.

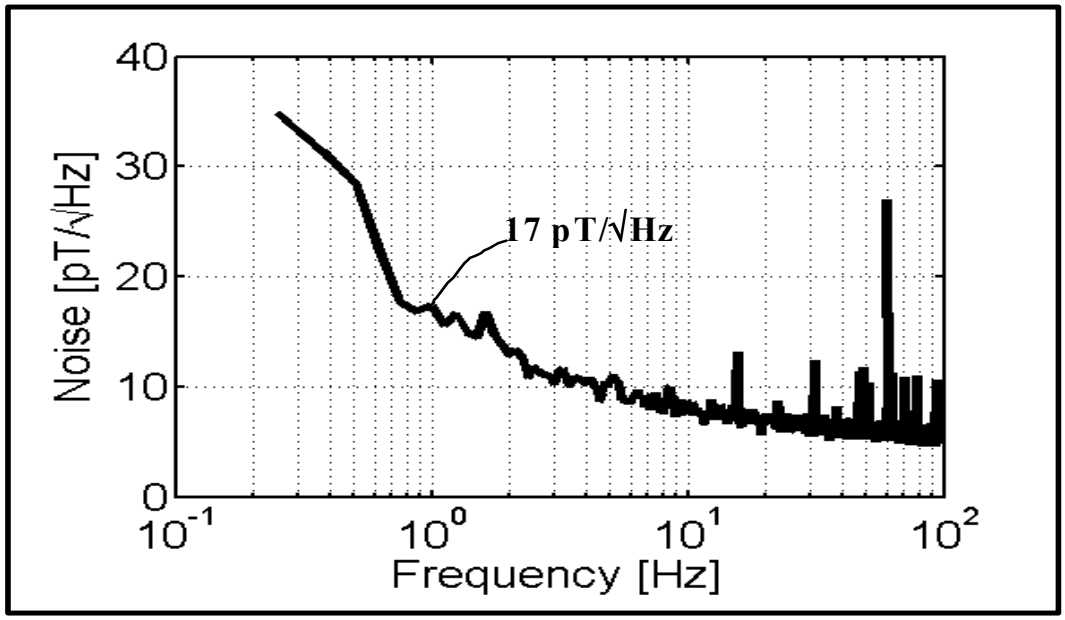

Fig. 18.. Representative noise spectrum from a ***B***-field sensing element of a TFM in a Grad-03-300L gradient sensor The data were taken with a HP3562A Dynamic Signal Analyzer to verify the manufacturer's published sensor-noise specifications. The TFM was inside a magnetically shielded enclosure inside a copper-plated shield room in the Magnetic Sensors lab at NSWC PCD. Each Grad-03-300L gradient sensor has two TFMs (separated by 30 cm). and a total of six *B*-field sensing elements with uncorrelated root mean square (rms) noise levels of ≤ 20 pT/√Hz at 1 Hz. A rule of thumb for fluxgate type sensor is that a sensor's peak to peak (pp) noise level is about six times its rms levels [15]. Since the STAR System takes ***B***-field data with little averaging, each of the STAR's ***B***-field sensing elements has a pp noise of about 120 pT/√Hz at 1 Hz. that is not correlated with the noise on the other channels. Thus, the instantaneous peak-to-peak noise level of each gradient component (obtained by taking the difference between two *B*-field channels) will be about 120 pT√Hz.

- A unique sensor support structure (SSS) (Fig. 11 in Materials and Methods Section) was designed and constructed at NSWC PCD. The SSS is made of very rigid and lightweight carbon fiber composites and its construction was finally completed in September 2006.
- A very critical part of the sensor's data acquisition system, namely a 6-channel, 24-bit Earth Data Ltd. Model PS6-24 Digitizer with a Garmin Model GPS 35-HVS Global Positioning System (GPS) was acquired on loan from Earth Data and integrated into a one-fourth subunit of the MagSTAR Sensor in July 2006.. The ¼ subunit was comprised by a Grad-03 sensor, an Earth Data Model PS6-24 6-channel digitizer (Fig. 10B) and an AMPRO single board computer (Fig. 12 (a).
- A MicroStrain Model 3DM-GX-1 orientation sensor/accelerometer (Fig. 13) was purchased, characterized and (in August/September 2006) integrated into the signal processing system of a ¼ subunit (see Fig. 14) of the prototype MagSTAR sensor.
- An Ampro Pentium III-based single-board computer (SBC) (visible in Fig. 12 (a)) was purchased and programmed to run a Linux/MatLab-based program for real time data processing and control of STAR sensor input/output (I/O) operations (July-August 2006).
- A very significant milestone was the development of a fully operational MATLAB-based software program for data acquisition, signal processing and I/O for the ¼ MagSTAR subunit in September, 2006. An improved version of this program is included in Appendix (B). In particular, a critical accomplishment for development of a truly practical tensor gradiometer was the development of a an effective signal processing algorithm for calibration of residual gradient channel imbalances and real-time motion noise compensation. With this achievement, a one-quarter subunit of the MagSTAR could be field-tested in motion without having to wait for delivery of long lead-time PS6-24 Digitizers.
- Final acquisition of all four PS6-24 Digitizers was finally completed and the digitizers were integrated into the STAR sensor in November-December 2006.
- A signal processing and control (SPAC) module (also known as "the electronics box" -Fig. 12(a)) comprising the AMPRO SBC, Input/Output (I/O) and control circuitry, power supply circuitry and lithium-polymer battery power for the entire MagSTAR system was completed in December 2006. The rechargeable batteries allowed completely autonomous (untethered) operation of the portable MagSTAR sensor system for about three hours.

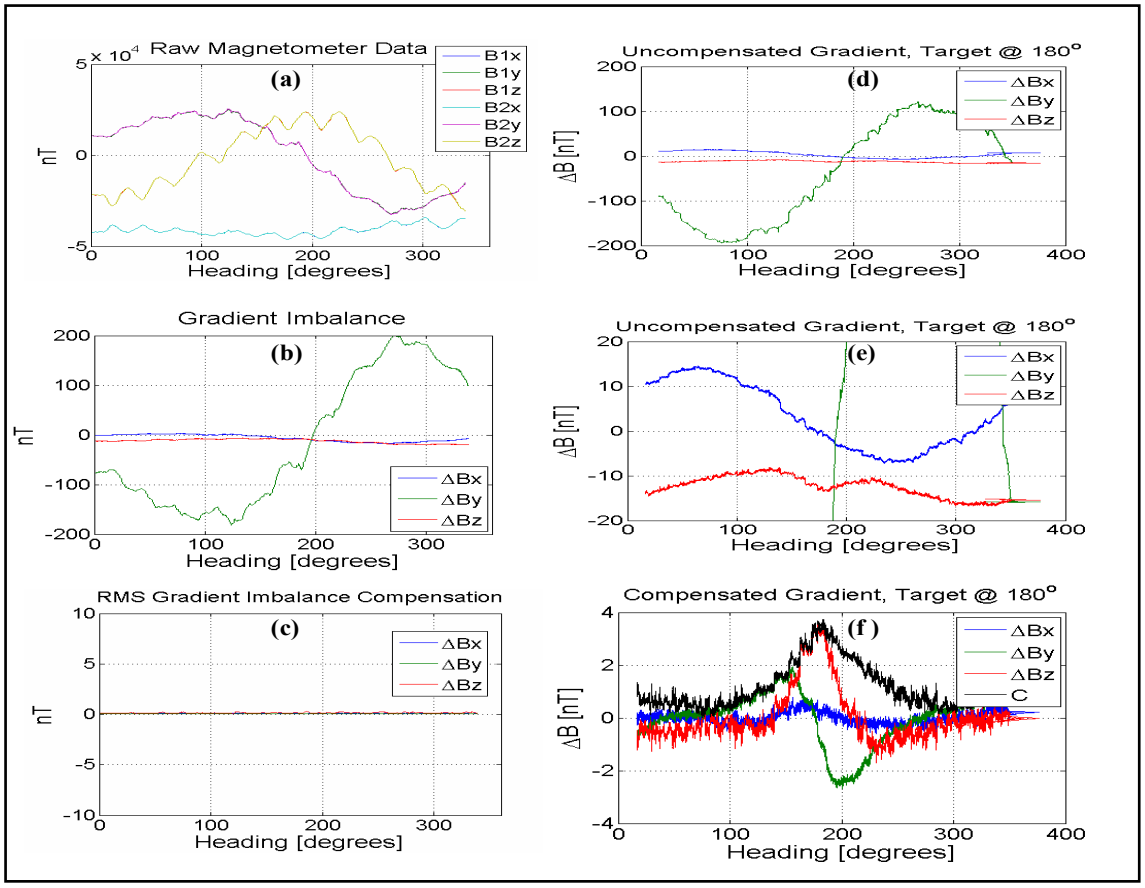

Fig. 19. Demonstration of reduction of motion noise effects and enhanced target-discrimination. The data are from field tests of a single-axis six-channel subset (comprised by a Grad-03-300L gradient sensor, a PS6-24 ADC and the STAR Gradiometer CPU (an Ampro Pentium III SBC).

The **(a), (b), (c)** data curves on the left side were taken as sensor pitch, yaw (heading) and roll were changed in a gradient-free zone. The data curves show: **(a)** Raw magnetic field measurements. (Only three curves are distinguishable because here on a scale of +/- 50,000 nT respective *B*-field curves e.g., B_{1X}, B_{2X}, etc., overlay each other.) **(b)** Calibration curves showing gradient imbalance errors that were input into the STAR sensor's motion noise compensation algorithm. **(c)** Results from self-consistent application of the STAR's motion noise correction algorithm to the data of (a) and (b). The gradient imbalance errors were reduced to about 0.25 nT peak to peak.

The **(d), (e), (f)** data curves on the right-hand side were taken as the calibrated sensor was swung at 3°/second on a 5-m diameter circular path. A 14.5 Amp-meter-squared magnetic dipole target was located at 180° and at a closest distance of 6.0 m. The data curves on the right show:

(d) Uncompensated gradient errors with the target signature buried in the sensor noise.

(e) Raw gradient data of d) on a ten times more sensitive scale but target signature is still not easily discriminated.

(f) Application of the MagSTAR's motion noise compensation algorithm allowed discrimination of the target gradient signature and calculation of a partial (three-component) *C*-parameter at sensor-target ranges of up to nine meters.

Results and accomplishments in 2007.

In 2007 the project accomplished the critical objective (and Go/No-Go milestone) of demonstration of proof-of-principle of the STAR concept for real-time, point-by-point DLC of magnetic targets. Subsequently, the R&D effort was directed toward the more open-ended objective of refinement and optimization of the prototype MagSTAR technology's hardware and software. A combination of hardware malfunctions and budgetary constraints slowed progress toward the end of FY07. For FY07, a little over one man-year of funding (i.e., $170K before "taxes" i.e., overhead, etc., of about 13%) was available. Consequently less than $150K could be directly used by the project and progress was delayed due to a lack of sufficient personnel assigned to the project's optimization effort. In addition to sensor-optimization effort, significant work was directed toward characterization and troubleshooting of sensor instability problems. Some of the hardware problems are described below. Nevertheless, as indicated below, significant progress was toward development of a truly practical and effective man-portable magnetic sensor technology for DLC of UXO.

The following list chronologically summarizes the project's significant results and accomplishments (and technical problems) in 2007.

- Improved software was developed in January-February 2007 to provide: a) error-handling routines to compensate for a data drop-out problem that afflicted the AMPRO SBC when running MATLAB to open RS 232 serial ports for data acquisition from the Digitizers, b) a Graphical User Interface (GUI) data display program to facilitate alignment and collimation of the gradient sensors in the Sensor Support Structure (SSS), c) A GUI for near real time display of target DLC parameters (range, bearing, elevation and magnetic signature) and user-friendly I/O to allow the MagSTAR operator to control and observe sensor system operation with a head-mounted display and a touchpad mouse.
- Alignment and collimation of the four Bartington Model Grad-03-300L gradient sensors in the Sensor Support Structure (SSS) using the "data_output display" subprogram of the main "super_STAR" program (Appendix (A). In order to minimize residual gradient imbalances all respective field sensing elements were mechanically aligned and collimated to within 0.4 degrees. (January 2007)
- A MicroOptical Model SV-6 heads-up display for real time display of target DLC parameters (i.e., range, bearing and magnetic dipole moment) that had been on order since 31 July, 2006 was finally received on 18 January, 2007 and integrated into the sensor system. Previously, the real-time data display of target parameters had been provided by a flat-panel display unit.
- Integration of all available subsystems and software into a fully operational prototype man-portable MagSTAR sensor (Fig. 20) (January 2007) .
- The first "Phase I" field tests of the complete MagSTAR sensor were very successfully performed in January 2007. Fig. 21 illustrates the basic test procedure. The operator simply moves the sensor system in the vicinity of a magnetic target and the MagSTAR automatically performs DLC of any magnetic target within its range.

Fig. 20. The prototype STAR Sensor being carried for field testing. A heads-up display unit and touchpad type mouse provides an intuitive, user-friendly Input/Output modality for control of sensor operation and a near real-time indication of the target's DLC parameters (i.e., range, bearing, elevation and. magnetic signature- Fig 22).

Fig. 21. Procedure for Phase I field tests.

- The MagSTAR's operator carries the sensor in the vicinity of a magnetic target (simulated here by the steel sphere on the right-hand side of the photo.
- The STAR sensor automatically measures, displays and stores the target's raw and processed DLC data in near real-time (≈ 3 s). The DLC data include GPS location and time information and can be played back for further analysis after testing is complete.

- Test and Evaluation. From January through May 2007, a series of field tests were performed against magnetic targets. Typically for these tests, as shown in Fig. 21, data were taken as the sensor system was hand-carried in the vicinity of a magnetic target. For convenience and to avoid potential naval security related problems that relate to the magnetic signature of real UXO-type objects, during these tests the target was a simple permanent magnet with a magnetic dipole moment of 14.5 Am^2 . The target produced a magnetic signature equivalent to that of a ferrous shell with a volume of 0.029 m^3 (that is, about one cubic foot). Fig 21 illustrates (using a simulated target) the basic procedure for testing the STAR sensor. Fig. 22 is a data set illustrating the sensor's high speed DLC capabilities.

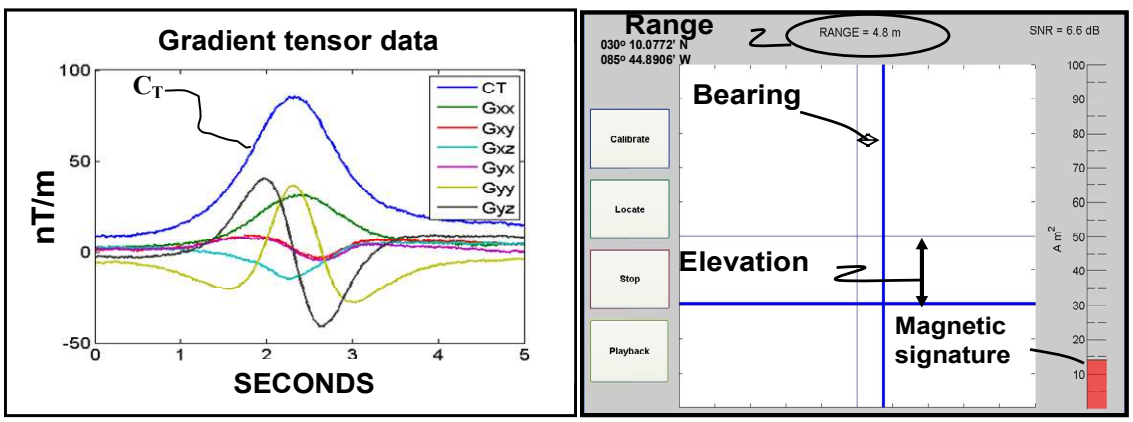

(A) **(B)**

Fig. 22. Magnetic gradient tensor data and screenshot from operator's display.

(A) High-speed, motion-noise-compensated gradient tensor (Gij) and tensor magnitude (C_T) data from one face one face of the sensor cube. The MagSTAR simultaneously develops six data subsets corresponding to the six faces of the cubic sensor array. (Figs. 23 and 24 show complete data sets.) Note, that the magnitude of the C_T-parameter is about 10 dB higher than the magnitudes of the individual G_{ij} components. The data were taken as the STAR Sensor was rapidly swung at about 40º/second in a 200° horizontal arc past a 14.5 Am^2 dipole target at a closest point of approach (CPA) of about 5 m. Ratios of C_T data from all six sensor-cube faces are used to triangulate target location $\boldsymbol{r}$ and the Gij data are used (in Eq. 2a) to calculate the target's magnetic dipole signature $\boldsymbol{M}$. The target's DLC data are saved in the sensor's compact flash memory and presented in near real-time (≈ 3s) on the operator's graphical user interface display shown in (B).

(B) Screenshot from operator's display corresponding to a data point from part (A). The screenshot shows an instantaneous location and the magnitude of the target's magnetic dipole signature as the hand-carried sensor was swept past the target. Range, magnetic signature and signal-to-noise ratio (SNR) are printed out. Blue crosshairs indicate the target's bearing and elevation relative to the sensor system's longitudinal symmetry axis (central black crosshairs). The virtual instrument buttons: Calibrate, Locate, Stop and Playback allow user-friendly control of sensor operation with a touchpad type mouse. If desired, the sensor's GPS coordinates can also be displayed.

In outline, the field tests consisted of the following:

(1) In a magnetic-gradient-free area of NSWC PCD's field test facility, the STAR Sensor was calibrated pressing the "Calibrate" button shown in Fig. 22 (B) and then (for two minutes) rotating the sensor in heading, pitch, and roll through 4π stereradians.

(2) The Sensor's gradient imbalance compensation calibration algorithm calculates a set of compensation coefficients that, as indicated in Fig. 19, for an ideally stable sensor (i.e., if the sensor holds its calibration) will reduce the gradient errors (and their associated motion noise errors) to approximately 0.25 nT.

(3) The operator uses a touchpad mouse to select the "Locate" mode (Fig. 22 (B)) and hand carries the STAR Sensor past a 14.5 Am^2 dipole target that is located in known positions within the field test range.

(4) As the sensor is carried past the target the sensor system automatically calculates and displays the target's location and magnetic signature. From January through May 2007 the field tests consistently demonstrated that:

- + The positions of the display unit's crosshairs correlated well with the target's position relative to the STAR Sensor's longitudinal symmetry axis.
- + The range to target that was calculated using the C_T parameters and the STAR Algorithm correlated very well with the true range.
- + The magnetic dipole signature calculated by the STAR Algorithm correlated very well with the target's true moment (the accuracy is particularly good at ranges of 5.5 m or less).
- + The STAR Technology will perform very well with no special constraints on sensor platform motion.
- + The STAR Sensor detected the target at distances of up to 7 meters; however, at maximum range the DLC performance was unstable. In particular wild fluctuations in the magnetic signature measurements were observed. As the target was approached sensor performance became stable and at about 5 meters performance was very robust.

Figs. 23 and 24 illustrate represent two complete sets of field data that were taken as the prototype sensor was swept past the project's standard. As discussed in detail in the figure captions the data (representative of many dozens of data sets) indicate problems with sensor system instabilities that result in reductions in the DLC range and accuracy of the prototype STAR sensor. In the course of MM-1511 the problems have been characterized and potential solutions have been identified and partially implemented. The problems need to fully addressed and solved in order for the STAR technology to reach its full potential for real time DLC of multiple targets in magnetically cluttered environments.

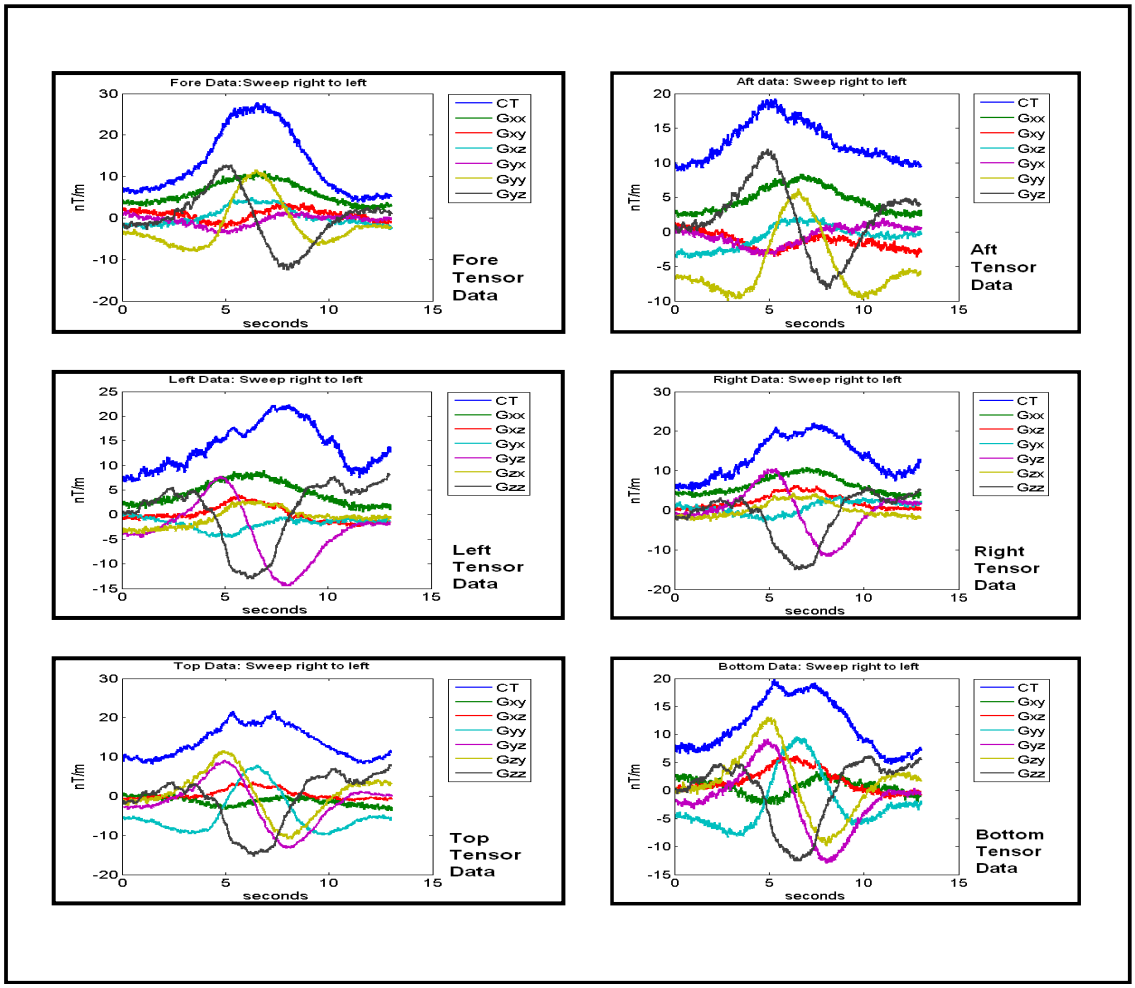

Fig. 23. Complete set of gradient tensor data (horizontal sweep past target). The data were taken as the hand-carried portable sensor was swept horizontally over an arc of about 200° past a 14.5 Am^2 magnetic dipole target located at a CPA of about 6 m. The STAR Algorithm uses the G_{ij} and C_T data to calculate a magnetic target's DLC data in near real time (≈ 3 s). The DLC data include GPS location and time info.

The following problems can be observed in the data: 1) An instability in Z-axis component G_{ZZ} of about 5 nT. In practice, this instability can reduces the sensor's effective DLC range to a little over 5 meters. 2) A difference of about 3 to 5 nT between pairs of theoretically symmetrical tensor components G_{XY} , G_{YX} ; G_{XZ} , G_{ZX} ; G_{YZ} , G_{ZY}.

These problems apparently result from mechanical instabilities/slippage in the alignment of the Grad-03 sensors in the sensor support structure. The design and construction materials of the sensor brackets in the SSS should be modified to preclude mechanical misalignments so that the improved MagSTAR will hold its calibration better and achieve a DLC range closer to the theoretical maximum.

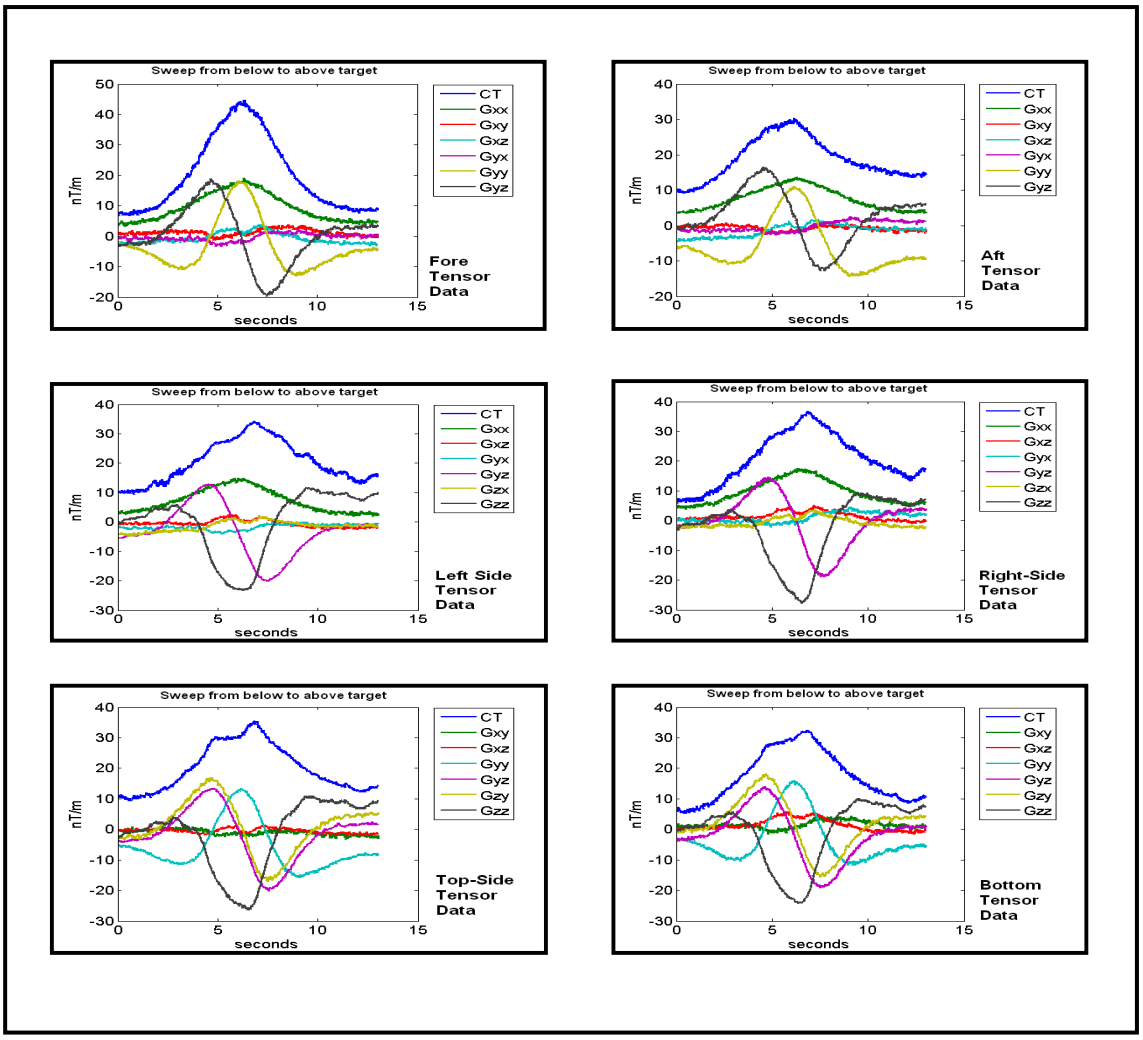

Fig. 24. Complete set of gradient tensor data (vertical sweep past target). The data were taken as the portable sensor was swept in a vertical arc of about 180° past a 14.5 Am^2 magnetic dipole target located at a CPA of about 5 m. Similar to Fig. 23, the data show a performance-limiting instability in tensor component G_{ZZ}. and a lack of complete symmetry between the tensor component pairs: G_{XY}, G_{YX}; G_{XZ}, G_{ZX}; and G_{YZ}, G_{ZY}.

In summary, the field test results clearly and unequivocally demonstrated proof-of-principle of the STAR concept and demonstrated the world's first man-portable magnetic sensor technology for real-time point-by-point Detection, Localization and Classification (DLC) of Unexploded Ordnance. However, engineering problems related to sensor system instabilities and drift cause a reduction of DLC range of about 40%, i.e., an actual range of a little over 5 m compared to the sensor's theoretical DLC range of up to 9 m for a 14.5 Am^2 target. Field test data indicate that the drift problem is partially related to changes in temperature and partially related to changes in mechanical alignment of the sensor array. These technical problems need to be addressed in order to increase the STAR Sensor's effective range and ability to perform effective DLC in magnetically cluttered environments. Other technical problems observed in 2007 and solved in FY07-08 are described below.

Problems in 2007.

The project made outstanding progress in the first two and one-half quarters of FY 07. However, starting in the late third quarter of FY07 the following hardware-related problems slowed progress toward optimization of the prototype sensor system:

1. In late May 2007, the STAR sensor's Pentium III-based AMPRO Single Board Computer (SBC) became unusable after its battery voltage dropped too low. The back-up SBC did not work properly in the field due to an intermittent problem with a serial (RS-232) data port. After some delays a software patch (using Universal Serial Bus (USB) ports alleviated (but did not completely resolve) the serial data problem
2. An intermittent malfunction in one of the magnetic field sensing elements of Bartington Model Grad-03-300L Gradiometer # 031 caused additional delays in the sensor optimization effort. Fig. 25 shows a time series of *B*-field data that captures the intermittent problem in one of the 24 channels of *B*-field data that are developed by the sensor. The sensor # 031 was returned to the manufacturer for repair and remained with the manufacturer in November and most of December 2007.

The following steps were taken to solve the above problems:

(A) An improved software solution for the AMPRO's serial communications problem was implemented and the AMPRO seemed to work OK albeit with occasional data dropouts.

(B) Based on the recommendations of NSWC PCD personnel with experience in SBC's, a WinSystems SBC–based signal processing system was developed to replace the marginally effective AMPRO unit. When mounted in its development kit, the WinSystems SBC seemed to work well with no serial communications problems and data dropouts only on system startup. However, when integrated into the MagSTAR's electronics box the WinSystems SBC unfortunately was too slow to run the MagSTAR Sensor's MATLAB-based STAR Algorithm and provide a near-real time display. Consequently, it became evident that an upgraded, more powerful SBC (with dual-core microprocessor) would be required to run the more advanced algorithms that are needed for multi-target discrimination.

(C) The Grad-03-300L gradiometer was returned for repair and recalibration by the manufacturer (Bartington Instruments).

(D)) A spare, backup unit of the Bartington Instruments Ltd. Model Grad-03-300L gradient sensor was ordered. The spare Grad-03 unit will help avoid future delays in sensor system optimization that could arise due to malfunction of a single unit of the STAR Sensor's four Bartington Model Grad-03-300L gradient sensors.

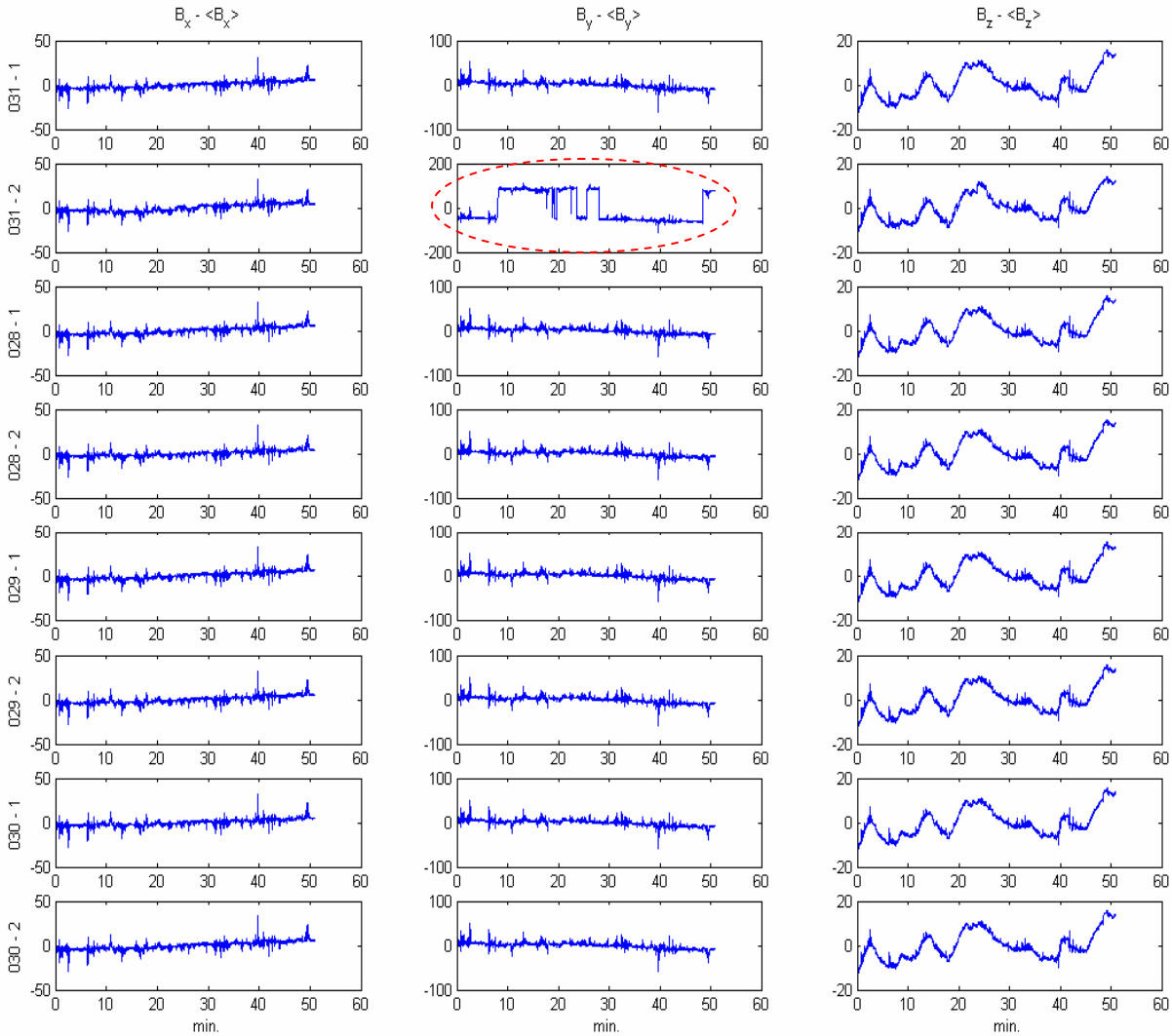

Fig. 25. Intermittent malfunction of a *B*-field-sensing element (B_Y sensing element #2 of Bartington Model Grad-03-300L serial number 031). The graphs represent 24 channels of *B*-field data that simultaneously were recorded over 50 minutes while the MagSTAR Sensor was stationary in a gradient-free area.

The graphs plot changes in *B*-field in nano tesla (nT) versus time in minutes. The numbers in the far left column refer to Bartington Model Grad-03-300L gradient sensors and their respective triaxial field sensing elements. For example, the numbers "031-1" refer to triaxial fluxgate magnetometer (TFM) #1 of gradient sensor serial number 031 and "031-2" means TFM #2 of gradient sensor #031. For all graphs, the units on the vertical scale are nano-tesla (nT). The graphs are arranged in three columns; each column represents a particular YXZ component of *B*-field minus the average value of that component. From left to right the columns represent, respectively: $B_X - \langle B_X \rangle$, $B_Y - \langle B_Y \rangle$ and $B_Z - \langle B_Z \rangle$. (Where $\langle B_X \rangle$ is the average value of B_X, etc.)

With the exception of the B_Y-field sensing element # 2 of gradient sensor #031, the measurements made by respective field-sensing elements are very well correlated. However, as indicated by the red dashed oval, the data from B_Y-field sensing element # 2 of gradient sensor #031 suffered random, step-function-like changes of about 100 nT. These random changes caused corresponding random changes in the sensor system performance.

Results and accomplishments in 2008

In 2008 the project focused on development of an improved technology (hardware and software) that would allow discrimination of UXO in magnetically cluttered environments. In 2007, malfunctions and limitations of the AMPRO and WinSystems SBC's had limited progress. Therefore, in 2008 the prototype MagSTAR's signal processing hardware was substantially upgraded with a much faster and more powerful dual-core SBC. Also, a more robust and reliable electronics box (Fig. 12(b)) equipped with greater-capacity lithium polymer batteries was constructed. Software was written for the new SBC and new STAR-type algorithms were developed for more accurate localization and classification of magnetic targets. In particular, since effective discrimination between UXO and clutter requires accurate measurement of a target's magnetic dipole signature, the new signal processing algorithms were developed to remove the STAR's asphericity errors and improve the accuracy of the STAR's magnetic signature measurements. Consequently, the prototype sensor was upgraded with:

1. A powerful, dual-core SBC.
2. Improved signal processing algorithms for: a) Removal of asphericity errors that limit the accuracy of magnetic signature measurements. b) More effective and accurate DLC for any sensor-target orientation, c) more effective discrimination of UXO in magnetically complex environments.

The basic STAR approach provides a very effective motion-noise-resistant technology for real-time DLC of magnetic targets. However, the prototype technology in 2006-2007 had several limitations with regard to accurate classification of UXO. In particular: 1) Maximum DLC accuracy required the sensor to be pointed at the target. 2) The process of determination of target signature $\boldsymbol{M}$ was subject to "asphericity errors" due to the C_T-fields' departure from perfect spherical symmetry [6,7], 3) The original STAR process has limited effective range in magnetically cluttered regions where there is significant overlap of anomaly fields from multiple targets. Since effective magnetic DLC of UXO crucially depends on the ability of a sensor technology to perform accurate determination of $\boldsymbol{M}$, in 2008 Project MM-1511 focused on improving the accuracy of its measurement process, in particular with regard to determination of $\boldsymbol{M}$-components

While substantial effort was directed toward solving some of the engineering problems (e.g. sensor system instabilities) that limit DLC range and accuracy, most of the progress in 2008 was made in the development of new signal processing hardware and software to enhance sensor system performance. Two new algorithms were developed for more accurate and effective localization and classification of magnetic UXO . Namely:

- A "Directional Derivative" (DD) method that uses differences between gradient tensor magnitudes to determine the vector components of a target's location and magnetic signature. The DD calculations are subject to asphericity errors; however, they provide very good seed parameter for a least squares fit based algorithm..
- A least-squares-fit (LSF) approach that uses the DD method's location and magnetic signature measurements in the gradient tensor equations (Eq. 2a) to develop a best least squares fit to the measured tensor component data.

The least squares fit approach is appropriate for non-cluttered environments characterized by single, spatially isolated targets while the Directional Derivative method has advantages for magnetically cluttered environments of the type represented

in Fig. 4. Both of the approaches will provide a calibrated readout in degrees of a target's bearing and elevation relative to the sensor system.

Directional derivative- and least squares-based STAR algorithms

In 2008 new and improved STAR algorithms were developed with the objective of the eventual development of signal processing modalities for DLC of UXO in magnetically cluttered environments. The improved algorithms based on "directional derivative" (DD) and least squares fit (LSF) approaches are described on page 22. The combined DD/LSF approach was developed to provide more effective and accurate DLC performance for any sensor-target orientation and to remove the asphericity errors that are inherent to the original STAR algorithm. In particular, the new algorithm provide much improved accuracy in the measurements of the 3-D components of a magnetic target's magnetic dipole moment vector. The following results from the first version of the combined DD/LSF algorithm results were presented in [13,14].

Field-test data showing results of application of improved DLC algorithm

Figs. 26-29 represent field test data showing the enhanced accuracy in measurement of components of M that is provided by the first implementation of the combined DD/LSF STAR algorithm. The improved algorithm was applied to field test data that were taken earlier by the MagSTAR sensor. However, the DD/LSF algorithm can readily be integrated into the sensor system's signal processing software and, thereby provide accurate near real time measurements of a UXO's location and magnetic signature. The results shown in Figs. 26-29 indicate that for a sensing platform in general unconstrained motion, the preliminary (i.e., not yet fully optimized "Version 1.0.0") DD/LSF algorithm can provide reasonably accurate measurements of target location $\boldsymbol{r}$ and magnetic signature $\boldsymbol{M}$. The algorithm rapidly converged (in just two iterations or cycles of the linear and non linear LSF process) to very near the true values of the vector components of target location r and magnetic signature $\boldsymbol{M}$ .in the sensor frame of reference. For a 14.5 Am^2 target, the preliminary DD/LSF algorithm will accurately determine components of $\boldsymbol{r}$ at ranges of up to 5 meters; however, at ranges greater than 4 meters the process results in unacceptably large errors in measurements of components of $\boldsymbol{M}$.

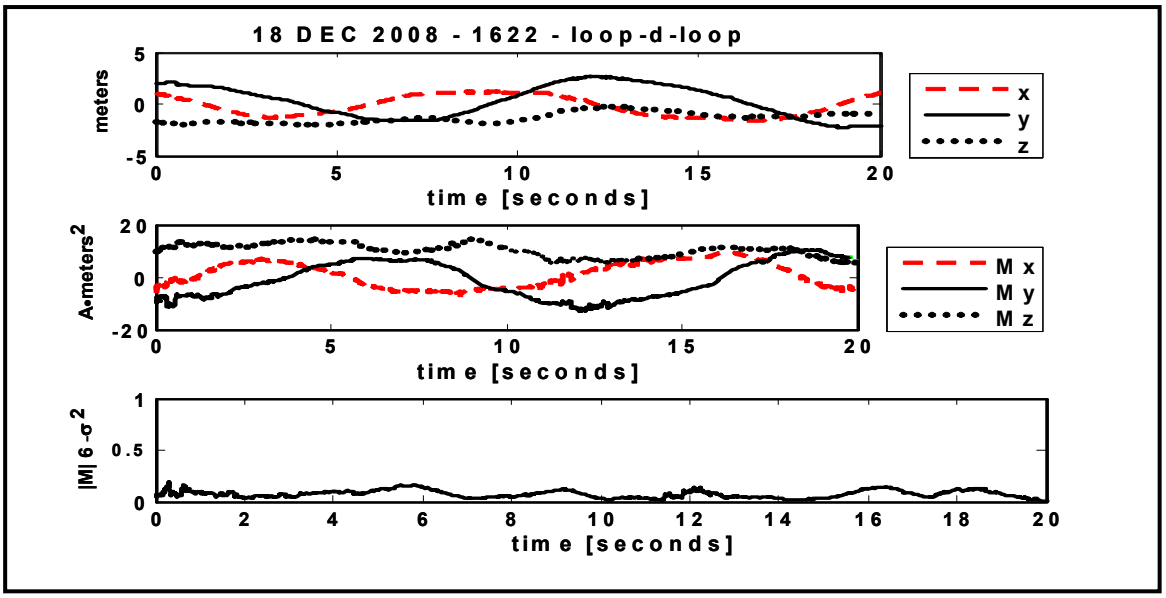

Fig. 26. Point-by-point values of target position (***r***) and magnetic signature (***M***) calculated using the DD/LSF algorithm. The algorithm was applied to field-test data that were taken as the hand-carried prototype Mag STAR sensor was moved at 25º/s in a 2 meter high by 5 meter wide rectangular path centered on a 14.5 Am^2 target located at a horizontal distance of about 3 to 4 m from the center of the vertical rectangle. The top graph shows target position coordinates denoted x, y, z**;** the middle graph M_X, M_Y, M_Z . The bottom graph shows the variance between values of $|\mathbf{M}|_I = [M_X^2 + M_Y^2 + M_Z^2]_I^{0.5}$ that were calculated for each the six (I = 1 thru 6) sensor-cube faces.

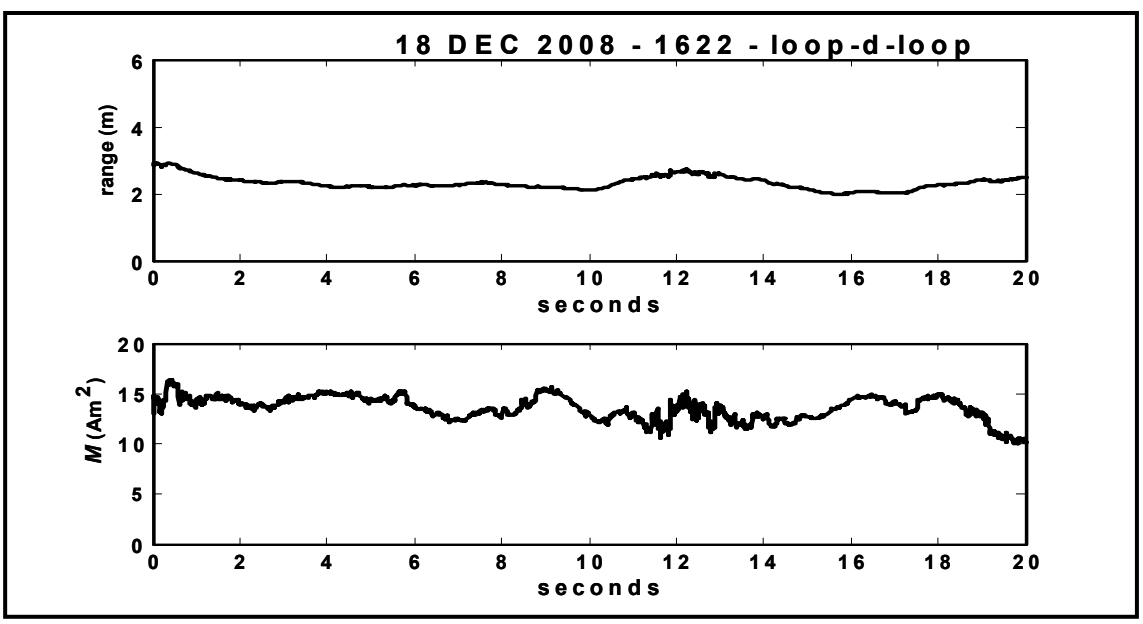

Fig. 27 Magnitudes of target range $|\boldsymbol{r}| = [x^2 + y^2 + z^2]^{0.5}$ (top graph) and magnetic signature $|M| = [M_X^2 + M_Y^2 + M_Z^2]^{0.5}$ calculated for the data of Fig. 26. The graph of $|\boldsymbol{r}|$ is a relatively stable and accurate; however the graph of $|M|$ shows substantial variation around the target signature's true value of 14.5 Am^2.

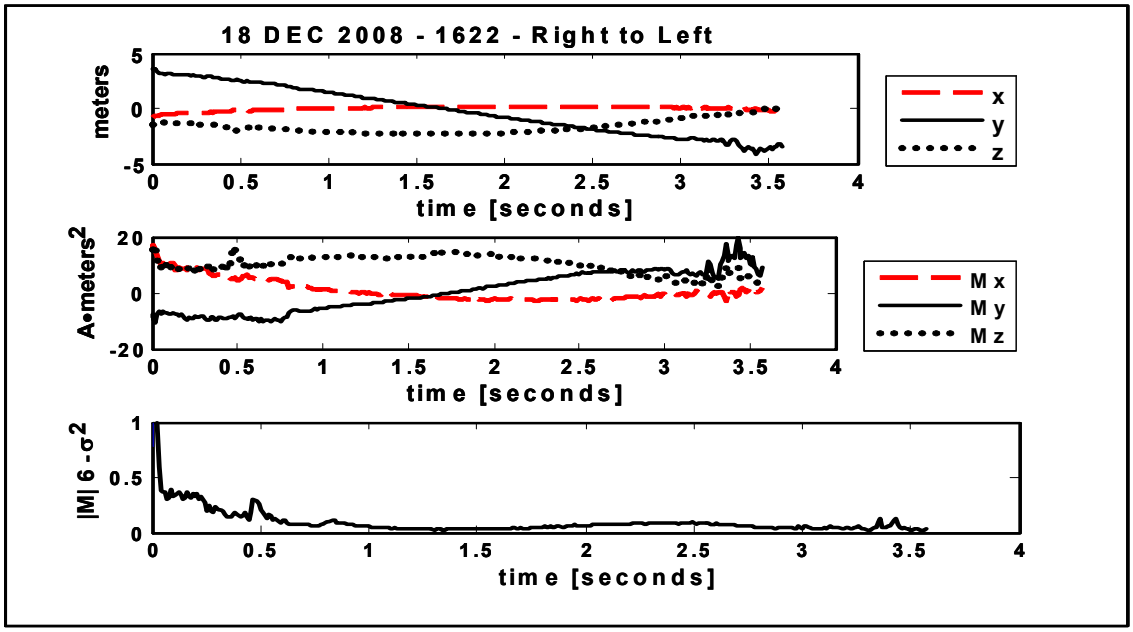

Fig. 28. Results from the application of a combined DD/LSF signal processing algorithm to field-test data were taken as the hand-carried prototype Mag STAR sensor was swept horizontally from right to left past a 14.5 Am^2 target located at about 4 m from the sensor). The top graph shows xyz coordinates of target location (in the sensor frame). The middle graph represents the sensor-frame values of **M**–components. The bottom graph represents the variance between the magnitudes $|\mathbf{M}|_I = [M_X^2 + M_Y^2 + M_Z^2]_I^{0.5}$ that the DD/LSF algorithm determined for each of the faces (I = 1 thru 6) of the sensor cube.

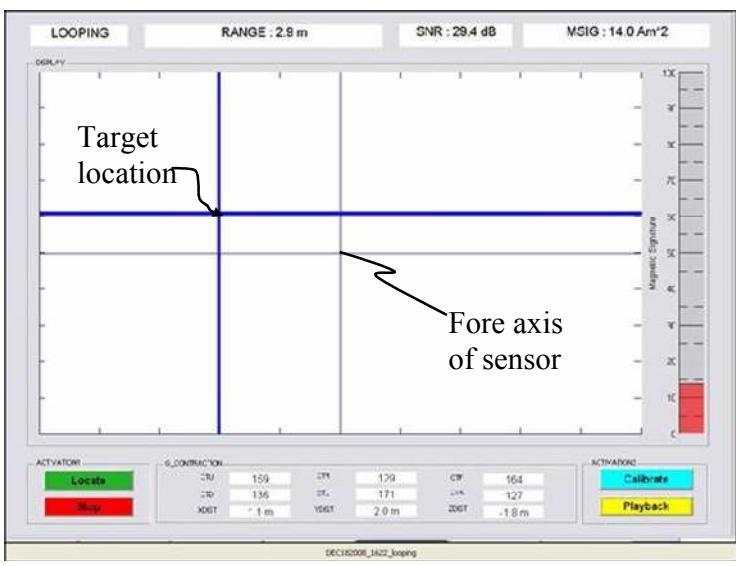

Fig. 29. Screenshot from operator's display (in "Playback " mode) showing a datapoint processed by a combined DD/LSF signal processing algorithm to field-test data. The data were taken as the hand-carried prototype Mag STAR sensor was swept at 25º/s in a 2 meter high by 5 meter wide rectangular path centered on a 14.5 Am^2 target located at a horizontal distance of about 3 to 4 m from the center of the rectangular path.

The observed ranges are about 50% below the range that should be provided by a more fully optimized version of the prototype MagSTAR sensor [6,7]. Thus, the data in Figs. 26-29 also indicate that further refinement and optimization of the DD/LSF algorithm is needed to improve the accuracy and effective range of the MagSTAR's DLC measurements. The algorithm is being perfected as part of an ongoing process aimed toward full development of the MagSTAR technology.

For the results shown here, the ***r*** and ***M***-components were calculated with respect the prototype system's sensor frame. However, in a more developed technology the Earth-frame components of ***M*** that are needed for more accurate target localization and discrimination would be determined by using a combination of GPS plus orientation sensor data to transform the components measured in sensor frame into the Earth-frame.

The increased accuracy and range that will provided by a fully optimized DD/LSF algorithm is required for improved discrimination of isolated targets and also for the achievement of the MagSTAR project's main objective: the development of a practical and effective sensor system for real-time "on the fly" detection, localization and classification/discrimination of UXO in magnetically complex environments.

Concluding Summary

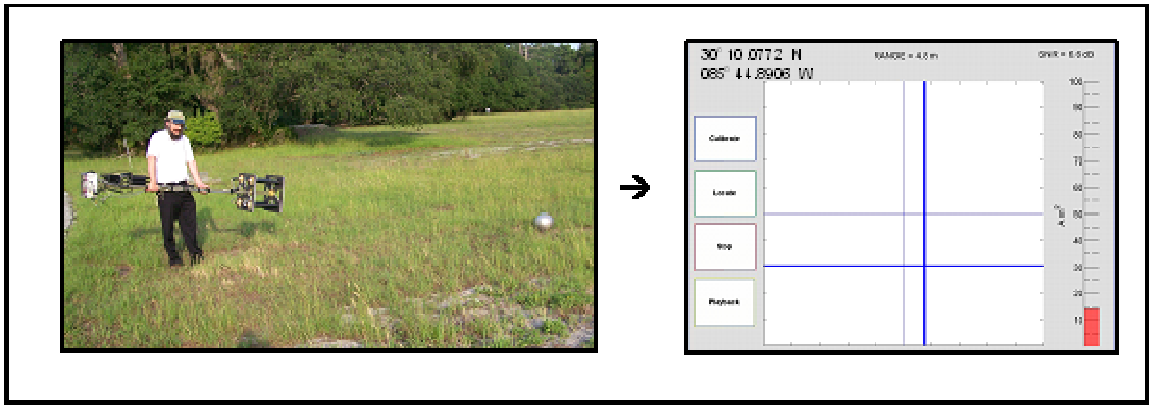

Fig. 30. Pictorial representation of the achievement of the project's original objective (illustrated in Fig. 1). A prototype man-portable magnetic STAR technology for near real-time, point-by-point DLC of UXO was developed and demonstrated.

In 2006 a working prototype of a man-portable magnetic sensing system based on a novel Magnetic Scalar Triangulation and Ranging (STAR) concept was designed, constructed and tested at Naval Surface Warfare Center Panama City. The STAR concept was created to provide a much more effective, motion noise resistant magnetic sensing technology for real time, point by point Detection, Localization and Classification/Discrimination (DLC) of UXO.

In 2007 field tests of the complete prototype STAR Sensor provided an excellent demonstration of the validity of the STAR concept and its unique advantages for highly mobile magnetic sensing platforms. In particular, the portable STAR Sensor, while being hand carried demonstrated real-time, point-by-point DLC of a 14.5 Am^2 magnetic dipole target. While in motion, the sensor system detected the target at distances of up to seven meters. At ranges of five meters, the sensor produced very accurate, near real-time (within three seconds) displays of target range, relative bearing and vector components of the target's magnetic dipole signature. The results of the project's ongoing field tests have provided a very strong proof-of-principle of the STAR concept and its advantages for highly mobile magnetic sensing systems.

In 2008 the project developed hardware, software and improved signal processing algorithms (i.e., the directional derivative and least squares method) for an improved STAR technology capable of discrimination of UXO in magnetically complex environments. Further optimization and testing of the upgraded man-portable STAR sensor is required. In particular, in order for the technology to achieve its full potential and transition to the user community the following should be addressed:

1. The STAR hardware and software should be further optimized to improve the technology's range, reduce the effects of residual sensor drifts, and improve the sensor's performance in a cluttered field of magnetic anomalies.
2. Field tests of the upgraded sensor system must be performed against real UXO-type targets in real-world environments.

References

[1] P. J. Carroll, J.F. McCormick. J.D. Lathrop, and D.C. Summey, , "Mobile Underwater Debris Survey System (MUDDS) Final Report, SERDP Project MM-52 (1998).

[2] L. Vaizer, J. Lathrop, and J. Bono, "Localization of Magnetic Dipoles" MTS/IEEE Oceans 2004-Techno-Ocean 2004 Conference Proceedings, pp869-873, (2004)

[3] R.F. Wiegert, US Patent 6,841,994, "Magnetic Anomaly Sensing System for Detection, Localization and Classification of Magnetic Objects."

[4] R.F. Wiegert, "Magnetic Anomaly Guidance System for Mine Countermeasures Using Autonomous Underwater Vehicles" MTS/IEEE OCEANS 2003 Conference Proceedings.

[5] R.F. Wiegert, J. Oeschger, and J.W. Purpura, "Magnetic Scalar Triangulation and Ranging System for Detection, Localization and Classification of Magnetic Targets", MTS/IEEE OCEANS-Techno-Ocean 2004 Conference Proceedings pp890-896, (2004).

[6] R.F. Wiegert and J. Oeschger, "Generalized Magnetic Gradient Contraction Based Method for Detection, Localization and Discrimination of Underwater Mines and Unexploded Ordnance. MTS/IEEE Oceans 2005 Conference Proceedings.

[7] R.F. Wiegert and J. Oeschger, "Portable Magnetic Gradiometer for Real Time Localization and Classification of Unexploded Ordnance, MTS/IEEE OCEANS 2006 Conference Proceedings (2006).

[8] R.F. Wiegert and J. Oeschger, "Demonstration of a Novel Man-Portable Magnetic STAR Technology for Real Time Localization of Unexploded Ordnance." MTS/IEEE OCEANS 2007

[9] J. D. Jackson, *Classical Electrodynamics*, John Wiley and Sons, Inc., New York, 1975.

[10] T.W. Altschuler, "Shape and Orientation Effects on Magnetic Signature Prediction for Unexploded Ordnance", UXO Forum 1996, (Williamsburg, VA, March 26-28, 1996), Conference Proceedings, pp.282-291.

[11] J. D. Lathrop, H. Shih, and W.M. Wynn, "Enhanced Clutter Rejection with Two Parameter Magnetic Classification for UXO", in Dubey, A. C., Harvey, J.F., Broach, J. T., and Dugan, R. E., (Eds), *Detection and Remediation Technologies for Mines and Minelike Targets IV,* The International Society for Optical Engineering, pp. 37-51, (1999).

[12] J. Vrba, "SQUID Gradiometers in Real Environments," in *SQUID Sensors: Fundamentals, Fabrication and Applications,*" H. Weinstock, (Ed), Kluwer Academic Publishers, Dordrecht, The Netherlands, (1996).

[13] R.F. Wiegert, K.H Lee and J. Oeschger, "Improved Magnetic STAR Methods for Real-Time, Point-by-Point Localization of Unexploded Ordnance and Buried Mines" in MTS/IEEE Oceans 2008 Conference Proceedings September (2008).,

[14] R.F. Wiegert, "Magnetic STAR Technology for Real-Time Localization and Classification" of Unexploded Ordnance and Buried Mines", 2009 SPIE Defense, Security and Sensing Conference; Proc. of SPIE, Vol. 7303 No. 66, (2009)

[15] P. Ripka, *Magnetic Sensors and Magnetometers*, Artech House, (2000).

Appendices

Appendix (A) List of Technical Publications. The following technical publications, presentations and patent applications were produced with support from SERDP Project MM-1511:

1. R.F. Wiegert and J. Oeschger, "Generalized Magnetic Gradient Contraction Based Method for Detection, Localization and Discrimination of Underwater Mines and Unexploded Ordnance". MTS/IEEE Oceans 2005 Conference Proceedings.
2. R.F. Wiegert and J. Oeschger, "Portable Magnetic Gradiometer for Real Time Localization and Classification of Unexploded Ordnance", MTS/IEEE OCEANS 2006 Conference Proceedings.
3. R.F. Wiegert, J. Oeschger, and E. Tuovila, "Demonstration of a Novel Man-Portable Magnetic STAR Technology for Real-Time Localization of Unexploded Ordnance," MTS/IEEE OCEANS 2007 Conference Proceedings.
4. R.F. Wiegert and J. Oeschger, "Man-Portable Magnetic STAR Technology for Enhanced al-Time Localization of UXO" Proc. 2007 UXO/Countermine/Range Forum
5. R.F. Wiegert and J. Oeschger, "Demonstration of a Novel Man-Portable Magnetic STAR Technology for Real Time Localization of UXO" Poster presentation at the National Defense Industrial Association (NDIA) 12-th Annual Expeditionary Warfare Conference Oct. 2007.
6. R.F. Wiegert and J. Oeschger, "Demonstration of a Novel Man-Portable Magnetic STAR Technology for Real Time Localization of UXO", Poster Presentation at 2007 SERDP Symposium "Partners in Environmental Technology" Conference December 5, 2007.
7. R.F. Wiegert, K.H Lee and J. Oeschger, "Improved Magnetic STAR Methods for Real-Time, Point-by-Point Localization of Unexploded Ordnance and Buried Mines" in MTS/IEEE Oceans 2008 Conference Proceedings September (2008).
8. R.F. Wiegert, K. Lee and J. Oeschger, "Man-Portable Magnetic STAR System for Real-Time Localization and Classification of Unexploded Ordnance" Invited presentation at 2008 SERDP-ESTCP Partners in Environmental Technology Symposium, December 2008.
9. R.F. Wiegert, K. Lee and J. Oeschger, "Improved magnetic STAR Methods for Real-Time, Point-by-Point Localization of Unexploded Ordnance and Buried Mines" Poster presentation at 2008 SERDP-ESTCP Partners in Environmental Technology Symposium, December 2008
10. R.F. Wiegert, "Magnetic STAR Technology for Real-Time Localization and Classification of Unexploded Ordnance and Buried Mines", Proc. of SPIE, Vol. 7303 No. 66, (2009)
11. R.F. Wiegert, "Improved Magnetic STAR Technology for Localization and Classification of UXO", Proceedings of the 2009 UXO/Countermine/Range Forum, August, 2009.
12. R.F. Wiegert, Patent: "Magnetic Anomaly Sensing-Based System for Tracking a Moving Magnetic Target", Patent issued March 2008; Application submitted to US Patent and Trademark Office (USPTO) in April 2006.
13. R.F. Wiegert and J. Oeschger, Patent Application: "Portable Magnetic Sensing System for Real-Time, Point-by-Point Detection, Localization and Classification of Magnetic Objects," Navy Patent Case 98,718. Application submitted to USPTO in September, 2007.
14. R.F. Wiegert and J. Oeschger, Patent Application: "Magnetic Anomaly Sensing System for Detection, Localization and Classification of a Magnetic Object in a Cluttered Field of Magnetic Anomalies", Navy Case 98,711 Application submitted to USPTO in April 2008. Note: the USPTO issued a "Notice of Allowance" that the patent will soon be issued.
15. R.F. Wiegert, Patent Application: "System and Method Using Magnetic Anomaly Field Magnitudes for Detection, Localization, Classification and Tracking of Magnetic Objects", Navy Patent Case 99,352 submitted to USPTO in February 2009.

Appendix (B) Computer program listings for man-portable MagSTAR sensor.

This appendix contains the complete code that was developed for operation of the man-portable MagSTAR sensor. The code includes data acquisition, signal processing (motion noise compensation, STAR DLC Algorithms, etc.) and sensor system I/O functions. One file is a MATLAB ".m-file" that can only be opened with MATLAB. For convenience, another file is a Microsoft EXCEL file. The program listings that are included with the Final Report for MM-1511 are:

1) "FRMM-1511v2_super_starJO12192008.m" a MATLAB file.
2) "FRMM-1511v2_super_starJO12192008.xls" a Microsoft EXCEL file.